



## UNITED STATES AIR FORCE RESEARCH LABORATORY

---

### Nonlinear Finite Element Modeling of an Airbag During Inflation and Impact

Xavier J. R. Avula  
Mathematical Modeling and Scientific Computing  
P. O. Box 31670  
St Louis MO 63131

Ints Kaleps  
Biodynamics and Acceleration Branch  
Biodynamics and Protection Division  
Human Effectiveness Directorate  
Wright-Patterson AFB OH 45433-7947

Prasad Mysore  
EASI Engineering  
2025 Concept Drive  
Warren MI 48091

March 1999

Interim Report March 1997 to December 1998

19991123 127

*Approved for public release; distribution is unlimited.*

Human Effectiveness Directorate  
Biodynamics and Protection Division  
Biodynamics and Acceleration Branch  
2800 Q Street BLDG 824 RM 206  
Wright-Patterson AFB OH 45433-7947

DTIC QUALITY INSPECTED 4

## NOTICES

When US Government drawings, specifications of other data are used for any purpose other than a definitely related Government procurement operation, the Government thereby incurs no responsibility nor any obligation whatsoever, and the fact that the Government may have formulated, furnished, or in any way supplied the said drawings, specifications or other data, is not to be regarded by implication or otherwise, as in any manner licensing the holder or any other person or corporation, or conveying any rights or permission to manufacture, use, or sell any patented invention that may in any way be related thereto.

Please do not request copies of this report from the Air Force Research Laboratory. Additional copies may be purchased from:

National Technical Information Services  
5285 Port Royal Road  
Springfield, Virginia 22161

Federal Government agencies registered with the Defense Technical Information Center should direct requests for copies of this report to:

Defense Technical Information Center  
8725 John J. Kingman Rd STE 0944  
Ft. Belvoir, VA 22060-6218

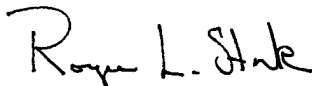
## TECHNICAL REVIEW AND APPROVAL

AFRL-HE-WP-TR-1999-0176

This report has been reviewed by the Office of Public Affairs (PA) and is releasable to the National Technical Information Service (NTIS). At NTIS, it will be available to the general public, including foreign nations.

This technical report has been reviewed and is approved for publication.

### FOR THE DIRECTOR



ROGER L. STORK, Colonel, USAF, BSC  
Chief Biodynamics and Protection Division  
Human Effectiveness Directorate  
Air Force Research Laboratory

# REPORT DOCUMENTATION PAGE

Form Approved  
OMB No. 0704-0188

Public reporting burden for this collection of information is estimated to average 1 hour per response, including the time for reviewing instructions, searching existing data sources, gathering and maintaining the data needed and completing and reviewing the collection of information. Send comments regarding this burden estimate or any other aspect of this collection of information, including suggestions for reducing this burden, to Washington Headquarters Services, Directorate for Information Operations and Reports, 1215 Jefferson Davis Highway, Suite 1204, Arlington, VA 22202-4302, and to the Office of Management and Budget, Paperwork Reduction Project (0704-0 188), Washington, DC 20503

1. AGENCY USE ONLY (Leave Blank)		2. REPORT DATE March 1999	3. REPORT TYPE AND DATES COVERED Interim Report March 1997 thru December 1998	
4. TITLE AND SUBTITLE Nonlinear Finite Element Modeling of an Airbag During Inflation and Impact			5. FUNDING NUMBERS C: F41624-95-C-6014 PE: 62202F PR: 7184 TA: 718443 WU: 71844301	
6. AUTHOR(S) Xavier J. R. Avula, Ints Kaleps, Prasad Mysore				
7. PERFORMING ORGANIZATION NAME(S) AND ADDRESS(ES) Mathematical Modeling and Scientific Computing P.O. Box 31670 St Louis MO 63131			8. PERFORMING ORGANIZATION REPORT NUMBER	
9. SPONSORING/MONITORING AGENCY NAME(S) AND ADDRESS(ES) Air Force Research Laboratory Human Effectiveness Directorate Biodynamics and Protection Division Air Force Materiel Command Wright-Patterson AFB OH 45433-7901			10. SPONSORING/MONITORING AGENCY REPORT NUMBER AFRL-HE-WP-TR-1999-0176	
11. SUPPLEMENTARY NOTES				
12a. DISTRIBUTION/AVAILABILITY STATEMENT Approved for public release; distribution is unlimited			12b. DISTRIBUTION CODE	
13. ABSTRACT (Maximum 200 words) In this study, a nonlinear finite element method was applied to the simulation of airbag deployment and contact with a solid body in a crash situation. A finite element model of the folded airbag was modified and the forces generated by an unfolding airbag during its impact with a rigid wall were investigated using DYNA-3D code. The finite element model was verified by comparing results with those reported in the verification of PAM-CVS code which couples the PAM-CRASH finite element code with the crash victim simulator CAL3D. Having verified the finite element model, the effect of airbag parameters on the acceleration of a rigid sphere resulting from contact with an inflating airbag was investigated. The parameters considered were fabric density, bag elasticity, input gas temperature and extent of venting. The influence of these parameters on the contact was significant: lowering the fabric density resulted in higher bag velocity which in turn resulted in higher rebound velocity; the lower the input gas temperature, the longer was the contact time and the lower rebound velocity. The acceleration and rebound velocity had an inverse relationship with vent area. These observations with additional studies could be used in the development of better occupant safety systems.				
14. SUBJECT TERMS Simulation, crash, safety, airbag, impact, finite element model			15. NUMBER OF PAGES 51	
			16. PRICE CODE	
17. SECURITY CLASSIFICATION OF REPORT Unclassified	18. SECURITY CLASSIFICATION OF THIS PAGE Unclassified	19. SECURITY CLASSIFICATION OF ABSTRACT Unclassified	10. LIMITATION OF ABSTRACT UNLIMITED	

**This Page Intentionally Left Blank**

## PREFACE

The project was conducted under the task "Modeling Airbag and Body Interactions" by the Biodynamics and Acceleration Branch, Biodynamics and Protection Division, Human Effectiveness Directorate, United States Air Force Research Laboratory, Wright-Patterson Air Force Base, Ohio and supported by Veridian, Inc. 5200 Springfield Pike, Suite 200, Dayton, Ohio. The simulations were performed by Mathematical Modelling and Scientific Computing Division of the Institute for Applied Sciences, St. Louis, Missouri.

This study was supported under Contract No. F41624-95-C-6014 with Veridian, Inc.

## TABLE OF CONTENTS

PREFACE.....	iii
LIST OF FIGURES.....	v
LIST OF TABLES.....	vi
ABSTRACT.....	1
INTRODUCTION.....	2
AIRBAG INFLATION PROCESS.....	4
AIRBAG MODEL FORMULATION.....	5
A. FABRIC MODEL.....	5
B. AIRBAG INTERIOR.....	5
C. EQUATION OF STATE; EVOLUTION OF GAS PRESSURE.....	8
AIRBAG SIMULATION.....	10
RESULTS AND DISCUSSION.....	13
A. VALIDATION OF THE AIRBAG MODEL.....	13
1. Pure Inflation.....	13
2. Impact Against Rigid Wall.....	14
B. PARAMETRIC STUDY.....	24
1. Effect of Fabric Density.....	34
2. Effect of Bag Elasticity.....	34
3. Effect of Input Gas Temperature.....	34
4. Effect of Venting.....	35
CONCLUSIONS.....	35
REFERENCES.....	44

## LIST OF FIGURES

Figure 1. Idealized Young's modulus as a function of fiber strain.....	6
Figure 2. Inflation of a folded airbag in different stages: (a) oblique view before deployment, (b) side view at 15 msec, (c) at 45 msec, (d) at 45 msec, and (e) at full inflation.....	15
Figure 3. Load curve for the input mass flow rate.....	16
Figure 4. Time history comparison of the airbag volumes.....	17
Figure 5. Time history comparison of the airbag pressures.....	18
Figure 6. Time history comparison of the temperature within the airbag.....	19
Figure 7. Time history comparison of the total mass of gas in the airbag during the period of simulation.....	20
Figure 8. Side view of the inflating airbag at 15 msec colliding with the rigid wall.....	21
Figure 9. Side view of the inflated airbag in contact with the rigid wall at 50 msec.....	22
Figure 10. Comparison of airbag volumes for the simulation involving the rigid wall.....	23
Figure 11. Comparison of airbag pressures for the simulation involving the rigid wall.....	25
Figure 12. Comparison of airbag temperatures for the simulation involving the rigid wall.....	26
Figure 13. Comparison of total mass of gas in the airbag or the simulation involving the rigid wall.....	27
Figure 14. Comparison of rigid wall z-forces for the simulation involving the rigid wall.....	28
Figure 15. Initial configuration of the folded airbag and the rigid spherical entity.....	29
Figure 16. Side view of the unfolding airbag and sphere travelling with constant velocity at 15 msec.....	30
Figure 17. Side view of the inflating airbag in contact with the rigid sphere at 40 msec.....	31
Figure 18. Side view of the rigid sphere penetrating the fully inflated airbag at 80 msec.....	32
Figure 19. Side view of the rebounding sphere and airbag regaining shape at the end of Simulation.....	33
Figure 20. Resultant acceleration and velocity time histories of the rebounding sphere for various fabric densities.....	36
Figure 21. Volume and pressure curves for the airbag for various fabric densities.....	37
Figure 22. Resultant acceleration and velocity time histories of the rigid sphere for different values of bag elasticity.....	38
Figure 23. Volume and pressure time histories for the airbag for different values of bag elasticity.....	39
Figure 24. Time histories of the resultant acceleration and velocity of the rigid sphere for a parametric variation of the input gas temperature.....	40
Figure 25. Time histories of the volume and pressure of the airbag for a parametric variation of the input gas temperature.....	41
Figure 26. Time histories of the effect of airbag venting on resultant acceleration and velocity of the impacting sphere.....	42
Figure 27. Time histories of the effect of airbag venting on volume and pressure of the airbag.....	43

## LIST OF TABLES

TABLE I: Material properties for the airbag fabric [12].....	11
TABLE II: Thermodynamic properties of the gas and ambient air [12].....	11



# **NONLINEAR FINITE ELEMENT MODELING OF AN AIRBAG DURING INFLATION AND IMPACT†**

Xavier J. R. Avula\*, Ints Kaleps\*\*, Prasad Mysore\*◇

\*Department of Mechanical and Aerospace Engineering and Engineering Mechanics  
University of Missouri-Rolla, Rolla, Missouri 65409-0050

\*\*AFRL/HEPA, Wright-Patterson Air Force Base, Ohio 45433-7901

## **ABSTRACT**

In this study, a nonlinear finite element method was applied to the simulation of airbag deployment and contact with a solid body in situations which may arise in survivable aircraft crashes. A finite element model of the folded airbag was modified and the forces generated by an unfolding airbag during its impact with a rigid wall was investigated using DYNA-3D code. The finite element model was verified by comparing the results with those reported in the verification of PAM-CVS code which couples the PAM-CRASH finite element code with the crash victim simulator CAL3D. Having verified the finite element model, the effect of airbag parameters on the acceleration of a rigid sphere resulting from contact with an inflating airbag was investigated. The parameters considered were fabric density, bag elasticity, input gas temperature and extent of venting. The influence of these parameters on the contact was significant: lowering the fabric density resulted in higher bag velocity which in turn resulted in higher rebound velocity of the sphere; fabrics of lower elasticity had shown increased contact time and higher rebound velocity; the lower the input gas temperature, the longer was the contact time and the lower the rebound velocity. The acceleration and rebound velocity had an inverse relationship with vent area. These observations with additional studies could be used in the development of better occupant safety systems for survivable aircraft crashes.

---

◇Present address: EASI Engineering, 2025 Concept Drive, Warren, Michigan 48091

†Sponsored by Human Systems Center (AFMC), Brooks Air Force Base, Texas under the task "Modeling Airbag and Body Interactions" supported by the Engineering Services Contract No. F41624-95-C-6014 with Systems Research Laboratories, Dayton, Ohio.

## INTRODUCTION

In vehicle crashes, injuries can be drastically reduced by minimizing occupant movement and subsequent impact with the vehicle interior. Passive supplemental restraint systems, which essentially consist of safety belts and airbags, are found to provide the best overall injury risk reduction. Viano [1] studied the fatality prevention effectiveness and biomechanical principles of different occupant restraint systems. In these systems, while the lap shoulder belts were found to provide the greatest safety, airbags were found to protect both belted and unbelted occupants. Digges [2] has examined the distribution of injuries to belted occupants involved in frontal crashes. These studies were consistent in showing that head and chest injuries were the most prominent in belted occupants. Injury patterns for the airbag restraints were also examined, but no patterns of serious injuries were observed with the use of airbags.

The study of air bag occupant restraint systems includes the study of the airbag materials, sensors, inflators, airbag folding and deployment patterns, and finally the interaction of the airbag with an articulated occupant model. In recent years, the finite element technique has been used widely in the automotive industry for modeling and simulation of airbag inflation and its interaction with an occupant dummy. The finite element computations are most convenient for generation of bag inertia forces and direct incorporation of material properties. In order to model the airbag inflation accurately, the finite element program should incorporate the gas dynamics during inflation. A gas inflation model based on the control volume concept couples the gas flow during the inflation process to the airbag structure. The model assumes that the gas is ideal with constant specific heats and that there is no heat transfer. Further, the temperature and pressure are uniform within the airbag. The thermodynamic aspects of the inflation model are documented in an article by Wang and Nefske [3]. These models require an input of mass flow rate and gas temperature data, which can be obtained from tank tests of an actual inflator. The simulations may be used to predict the occupant loads, acceleration levels, injury indices and other severity measures which help identify the crash-injury protection afforded to the occupant by the vehicle restraint system.

Nieboer [4] modeled inflated airbags with different kinds of boundary constraints associated with striking by impactors of different shapes and travelling at different velocities. Higher strain

levels and increased penetration were observed with higher impact velocities. It was found that for larger impactor forces, the individual bag volume and contact force curves tended to have similar shapes during penetration. Also the impactor shape and size were found to influence the airbag deployment pattern. These observations are important to the simulation of airbag-occupant interactions when the occupants are of different sizes and shapes as in the case of females and children.

The most important aspect of airbag simulation is the prediction of occupant dynamics caused by the contact and interaction between an inflating airbag and the occupant. In an impact simulation involving an occupant in the driver's seat, the occupant contacts the airbag about 30 to 40 milliseconds after the airbag deployment is initiated, which is adequate time for the airbag to assume full shape and volume. In these situations, the pre-deployment folding pattern of the airbag does not influence occupant response. In such simulations, the initial folding configuration of the airbag can be unfolded to assume a flat geometry for ease of model creation and faster computation time. For a simulation of a normally seated occupant impacting an inflated airbag with an initially unfolded airbag configuration is not a compromising simplification if the airbag is fully inflated before contact is made and there is no possibility of the folded lobes striking the occupant during opening.

Another type of simulation involves cases wherein the occupant is seated with his upper torso leaning on the steering hub or in another out-of-position orientation. In such cases, the occupant would be in contact with the airbag during the early stages of deployment. In these situations, the pattern of the airbag unfolding could have a significant influence on occupant injury. Therefore, in simulations involving an out-of-position occupant, one should include the folding configuration of the airbag and investigate the effects of early interaction with the occupant due to the unfolding of the airbag. Lakshminarayan [5], Lasry [6] and Khalil et al. [7] have investigated the inflation of a folded airbags and resultant interactions with an occupant. Yang [8] has studied the forces between the occupant and airbag for two different folding configurations and two different airbag mounting angles.

Presently, most automotive design processes integrate the analysis of the vehicle structure, vehicle interior components (steering wheel, instrument panel, etc.), restraint system, and the

occupants. This is achieved by coupling structural finite element programs with biodynamic modeling programs.

Apart from the automotive industry, research on occupant simulation is being conducted in the aerospace industry to investigate the possibility of incorporating airbags in large aircraft and helicopters. The purpose is to provide maximum protection to the pilot and other crew members during survivable crashes. As in automobiles, deployment time for different folding configurations and various airbag parameters are of interest. The aim is to minimize the relative velocity of the body at the time of impact with internal vehicle components.

In this work, an attempt has been made to simulate the deployment of an initially folded airbag and predict the contact forces between a solid object that represents a particular part of the occupant's body and the airbag during the unfolding phase and after full inflation. A review of literature indicates that the influence of airbag parameters such as airbag fabric density, elasticity, input gas temperature, and extent of venting on contact force is worth investigating. In the present investigation, a parametric analysis was carried out to calculate the airbag response and resulting acceleration of a rigid sphere after impact with a deploying airbag.

## **AIRBAG INFLATION PROCESS**

The automotive driver's side supplemental inflatable restraint system module consists of an inflator, which produces a gaseous filling medium, and a circular fabric bag housed in the steering column. In some recent and luxury models, in addition to the frontal impact airbag on the driver's side, airbags are installed on passenger's side above or below the glove compartment, and in the front doors to protect from side impact. The air bag material is woven nylon with self-venting pores or mechanical vents. The air bag equipment includes a diagnostic system which serves three functions: it monitors the air bag system, acts as a backup against electrical power failure, and performs readiness test at engine start-up.

The inflator produces nitrogen gas by igniting a material such as sodium azide ( $\text{NaN}_3$ ). This material is mixed with certain proprietary oxidizers and binding agents so that the non-volatile byproducts form a slag which is removed by filtration. Ignition of the mixture is facilitated by use of a highly exothermic and easily ignitable substance such as boron potassium nitrate ( $\text{BKNO}_3$ ).

In order to achieve proper sequencing of combustion in the airbag inflation process, the two pyrotechnic materials are contained in separate chambers. Orifices at the exits of each of these chambers and a third chamber, which contains both a slag trap and a filter, control the gas flow rates. The filter in the third chamber consists of knitted and compacted wire mesh, screen or fibrous material. The function of this filter is to prevent droplets and condensed particulates from entering the gas stream that inflates the airbag. In the process, the gas stream loses a significant amount of heat.

The airbag inflation process is initiated by using multiple crash sensors located remotely from the passenger compartment. The sensors detect rapid deceleration, as in a collision, and send an electric signal to trigger the inflator. In an automobile, the sensors are located such that a collision within a  $60^\circ$  arc in front of the vehicle triggers the inflator. After the sensors initiate inflation, the air bag is filled with gas to full inflation and then deflates as the gas escapes through vents.

Since the deployment of the airbag should occur fast, in 30 to 40 milliseconds, to fully inflate it in a very short time, the mass flow rate must reach high values quickly.

## **AIRBAG MODEL FORMULATION**

The airbag model formulation involves three aspects, namely:

- 1) Airbag fabric material characterization,
- 2) Modeling of the gas inside the airbag, and
- 3) Equation of state that describes the evolution of the gas pressure as a function of temperature and density.

### **A. FABRIC MODEL**

The fabric material model used in the airbag analysis is described in the LS-DYNA3D theoretical manual [11]. The fabric exhibits a strong material nonlinearity and cannot sustain compressive and bending stresses. Further, only low levels of stresses are developed in the fibers until the material is stretched taut, which means there exists an initial slack.

This behavior has been modeled by representing the modulus of the fiber as a function of fiber strain. The idealized model shown in Figure 1 produces a zero modulus for compressive strains (segment 1-2) and piecewise linear modulus for tensile strains (2-3-4). The segment 1-2 simulates the inability of the fibers to carry compressive stresses, and the segment 2-3-4 simulates the initial fabric slack.

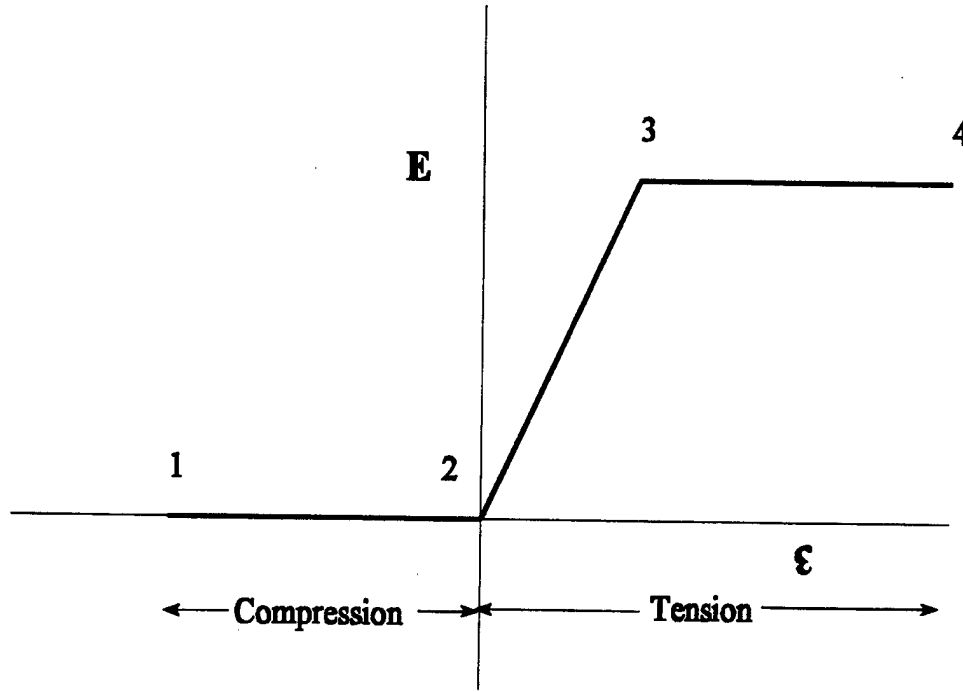


**Figure 1.** Idealized Young's modulus as a function of fibre strain

For the implementation of the material model, the Cauchy stress tensor  $\sigma_{ij}$  and the deformation tensor  $d_{ij}$  are transformed into the material coordinate system denoted by the subscript  $L$ . Then the stress state is incrementally updated in the material coordinates by;

$$\sigma_L^{n+1} = \sigma_L^n + \Delta \sigma_L^{n+\frac{1}{2}} \quad (1)$$

where,

$$\Delta \sigma_L^{n+\frac{1}{2}} = \begin{bmatrix} \Delta \sigma_{11} \\ \Delta \sigma_{22} \\ \Delta \sigma_{12} \\ \Delta \sigma_{23} \\ \Delta \sigma_{31} \end{bmatrix} = \begin{bmatrix} Q_{11} & Q_{12} & 0 & 0 & 0 \\ Q_{12} & Q_{22} & 0 & 0 & 0 \\ 0 & 0 & Q_{44} & 0 & 0 \\ 0 & 0 & 0 & Q_{55} & 0 \\ 0 & 0 & 0 & 0 & Q_{66} \end{bmatrix} \begin{bmatrix} d_{11} \\ d_{22} \\ d_{12} \\ d_{23} \\ d_{31} \end{bmatrix}_L \Delta t . \quad (2)$$

The terms  $Q_{ij}$  are defined as

$$Q_{11} = \frac{E_{11}}{1 - \nu_{12}\nu_{21}}, \quad Q_{22} = \frac{E_{22}}{1 - \nu_{12}\nu_{21}}, \quad Q_{12} = \frac{\nu_{12}E_{11}}{1 - \nu_{12}\nu_{21}}, \quad Q_{44} = G_{12}, \quad Q_{55} = G_{23}, \quad Q_{66} = G_{31} \quad (3)$$

Due to symmetry,

$$\nu_{21} = \nu_{12} \frac{E_{22}}{E_{11}} \quad (4)$$

where  $\nu_{ij}$  is Poisson's ratio for the transverse strain in  $j$ th direction for the material undergoing stress in the  $i$ th-direction,  $E_{ij}$  are the Young's moduli in the  $i$ th direction, and  $G_{ij}$  are the shear moduli. After completion of the stress update, the stresses are transformed back into the local shell coordinate system.

Also, due to thermodynamic considerations, the following constraints are enforced at each time step:

$$|\nu_{12}| < \sqrt{\frac{E_2}{E_1}} \quad |\nu_{21}| < \sqrt{\frac{E_1}{E_2}} . \quad (5)$$

## B. AIRBAG INTERIOR

The interior of the airbag could have been modeled by discretizing its domain using solid elements. The pressure-volume relation of the airbag would then be the sum of all elemental contributions. But this approach is numerically expensive and time consuming during the inflation phase of the airbag deployment and while the model is being refined.

A less computationally demanding approach for modeling the contents of the airbag is the control volume approach. A control volume is defined as the volume enclosed by a surface called the control surface. In the present case, the control surface is the airbag fabric and the gaseous interior is the control volume. As the evolution of the control surface is known, i.e. the position, orientation and current surface area of the airbag elements, the control volume can be calculated by applying Green's theorem,

$$V = \oint \bar{x} \cdot \bar{n} d\Gamma = \sum_{i=1}^N x_i n_{ij} A_j \quad (6)$$

where,

$V$  = control volume,

$N$  = number of elements,

$d\Gamma$  = elemental surface area enclosing the volume,

$x_i$  = average distance for each element  $A_i$ ,

$n_{ij}$  = direction cosines of the unit normal of the  $j$ th element with respect to the coordinate axes

$A_j$  = the surface area of the element  $j$ .

The above equation is integrated with respect to the direction of integration chosen to be parallel to the maximum principal moment of inertia of the surface.

## C. EQUATION OF STATE; EVOLUTION OF GAS PRESSURE

The pressure history in the airbag corresponding to the control volume is determined from an equation of state. The equation of state used for airbag simulation relates the pressure to the gas density (mass per unit volume) and the specific internal energy of the gas.



The gamma law equation of state as described in [3] is used to determine the pressure in the airbag:

$$P = (\gamma - 1)\rho e \quad (7)$$

where  $P$  is the pressure,  $\rho$  is the density,  $e$  is the specific internal energy of the gas, and  $\gamma$  the ratio of the specific heats is

$$\gamma = \frac{C_p}{C_v} . \quad (8)$$

The specific internal energy evolution equation corresponding to two states is given by

$$e_2 = e_1 [v_2 / v_1]^{(1-\gamma)} . \quad (9)$$

in which  $v_1$  and  $v_2$  are the specific volumes at two different states. The time rate of change of mass flowing into the bag is given by the law of conservation of mass;

$$\frac{dM}{dt} = \frac{dM_i}{dt} - \frac{dM_o}{dt} \quad (10)$$

where,  $M_i$  is the mass flowing into the airbag and  $M_o$  is the mass flowing out of the airbag.

This formulation is described in the LS-DYNA3D software [12] for modeling the airbag and its interior. Numerical results for the airbag model were calculated using the four-noded quadrilateral membrane shell element described in [12].

## AIRBAG SIMULATION

The airbag simulation was carried out using the explicit nonlinear finite element program LS-DYNA3D. The dynamic nature of crashworthiness contact problems, like airbag deployment combined with their complex geometry and highly nonlinear material behavior, makes them well suited for analysis using LS-DYNA3D.

A typical driver side airbag of 720 mm diameter with 2 vent holes of 20 mm diameter was studied. The airbag was modeled using special fully integrated membrane elements in conjunction with the fabric material model. The fabric material model was chosen over the orthotropic material model as it was found to be less time-step sensitive compared to the other models presented in the menu of models in LS-DYNA3D [12]. The membrane element was found to be especially suitable for anisotropic fabric behavior and the wrinkling phenomenon. Though fabric material models are unable to support buckling due to compressive stress, the "no compressive stress" option was not used as wrinkling normally occurs in airbags. Damping was used in the fabric material model to reduce the excessive distortions caused by the large amounts of energy input to the bag. The numerical values used for the material and geometric parameters of the fabric material are given in Table I [12]. The computed mass of the airbag was 292 gm.

The airbag was folded using the folding option in the LS-INGRID mesh generator. The airbag was initially discretized as two separate layers using this mesh generator. The location of fold lines, direction of fold, folding radius and sequence of folds were specified in the input file. The nodal point locations were then checked to avoid element interpenetrations after folding. A series of thick folds were defined in the folding operation. The airbag model included 1496 quadrilateral membrane elements. The larger number of elements was needed in order to model the folded configuration. The orientation of the bottom fabric layer was at  $0^\circ$  and  $90^\circ$ . For the top layer it was  $-45^\circ$  and  $45^\circ$ , as in an actual bag. A sequence of symmetric accordion folds perpendicular to the x-axis and a series of rolling and accordion folds about the y-axis were executed for the folds.

The equation of state from the Wang-Nefske airbag model [3], based on the control volume approach, was used to model the thermodynamic behavior of the gas flow into the airbag. It was assumed that the gas behaved as an ideal gas, and that the process was adiabatic, and the pressure

TABLE I: Material properties for the airbag fabric [12]

Parameter	Variable	Units	Value
Thickness	$t$	mm	0.35
Density	$\rho_{\text{fabric}}$	$\text{kg/m}^3$	1000
Young's Modulus	$E$	$\text{N/m}^2$	$1.0 \times 10^8$
Poisson's Ratio	$\nu$	-	0.4

and temperature were distributed uniformly throughout the control volume. For a given inflator, the heat capacities at constant volume and pressure, temperature of the gas, ambient density and pressure, load curve for the mass flow rate and a mass-weighted damping factor were specified. The numerical values for the above are presented in Table II. The input gas temperature was considered to be constant with time. The outflow of the gas was defined by an exit hole coefficient of discharge and exit area. A load curve was defined for the mass flow rate. The volume occupied by the gas was continuously monitored by calculating the volume of the finite element model of the airbag surface. Thus, knowing the volume occupied by the gas, the internal pressure was calculated from thermodynamic equations. This pressure was in turn applied to the finite element model to obtain the new bag shape and volume. This interchange between the gas model and finite element model provides the coupling between the two models.

TABLE II : Thermodynamic properties of the gas and ambient air [12].

Material	Parameter	Variable	Units	Value
Nitrogen	Specific heat at Constant Volume	$C_v$	$\text{J/kg}^\circ\text{K}$	741.0
	Specific heat at Constant Pressure	$C_p$	$\text{J/kg}^\circ\text{K}$	1038.0
	Temperature	$T$	$^\circ\text{K}$	700.0
Air	Density	$\rho_{\text{air}}$	$\text{kg/m}^3$	1.0
	Ambient Pressure	$P_e$	Pa	1.0E05

As the airbag inflates, a considerable amount of energy is transferred to the surrounding air. This energy transfer decreases the kinetic energy of the bag as it inflates. In the control volume concept, this was simulated by using the mass-weighted option.

A slideline is a contact algorithm to model the mechanical interaction between two bodies or two parts of the same body. During the inflation stage of an airbag, surface folds come into contact with themselves while unfolding. To eliminate the interpenetration between the surface nodes during inflation, an airbag single surface slideline specially developed for airbags was used. The single surface slideline is based on a penalty formulation. For a single surface algorithm, a master surface need not be defined.

In this study the impact of an airbag with a rigid wall and with a solid sphere were simulated. The results of the former problem were compared with those reported in the experimental verification of PAM-CVS code which couples with PAM-CRASH finite element code with the crash victim simulator CAL3D. After this verification, the impact of a rigid sphere with an inflating airbag was simulated. In both cases, the evolution of volume and pressure of the airbag was studied for various parametric changes in fabric density, bag elasticity, input gas temperature, and vent size.

To study the contact with a solid object, a sphere of 100 mm radius weighing 4.9 kgs initially at a center distance of 800 mm from the folded airbag was considered. The geometric contact entity approach was used to model the impacting sphere. Using the geometric contact entities for modeling contact of curved rigid bodies impacting deformable surfaces requires much less storage and vastly reduced the computational time in comparison with the more general faceted contact which requires defining master and slave surfaces. The geometric contact entity was developed using a solid modeling approach described in [7, p. 264]. For the contact phase, the nodes of the airbag were slaved to the impacting sphere. The simulation was carried out until 120 milliseconds and the results were post-processed.

## RESULTS AND DISCUSSION

### A. VALIDATION OF THE AIRBAG MODEL

For the purpose of verifying the airbag model, the cases of pure inflation of the airbag and its impact with a rigid wall were considered, and the results were compared with those obtained using the model of a generic driver side airbag from reference [13].

#### 1. Pure Inflation

In this section is described the simulation of the unfolding and inflation of an airbag starting from its initial folded position. Figure 2 shows the configurations of the airbag at different stages of inflation. For the first 25 milliseconds, the airbag was in the unfolding process. After this, the bag started to undergo rapid deformation due to the high momentum. By 45 milliseconds, the bag started to assume an ellipsoidal shape by which time the bag was fully inflated. Figure 2-(c) shows a fully inflated airbag. The wrinkling was caused by the expansion of the airbag in the z-direction. The wrinkling phenomenon in the present simulation was far less than that in a real airbag because of the smaller number of elements used to save computational time.

Figure 3 shows the input mass flow curve used in the simulation. The computed bag volume, bag pressure, gas temperature within the bag and the total mass of gas in the airbag which were compared with the similar data from reference [13] are shown in Figures 4 - 7. The control mass flow rate curve being the one in Wang-Nefske model (see Ref. [3]), the two curves in these figures illustrate similar trends and reasonably close agreement.

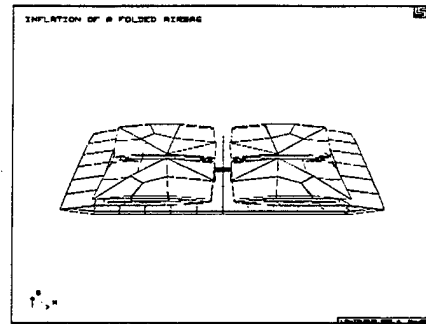
The computed peak volume of 62.5 liters attained at 60 milliseconds in the present simulation compared well with the volume measurements for an actual driver side airbag which varies from 62 to 68 liters. The high initial pressure was due to the gas flowing rapidly into the small volume of the folded airbag which resisted the expansion. Both the curves exhibited an initial peak at about 8-10 milliseconds. At the end of the simulation, both the curves had identical residual pressures. The total mass of gas within the airbag at 40 milliseconds was relatively higher which was again attributed to the difference in mass flow rates between the two models. The temperature curves were in very good agreement throughout the simulation. It must be noted that while the input temperature was assumed constant with respect to time, the gas temperature in the expanding airbag will vary in accordance with the gas law.

## 2. Impact Against Rigid Wall

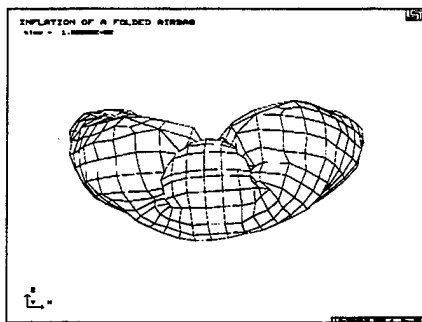
In this section is presented an aspect of model verification based on correlation between the contact forces generated during the airbag deployment against a rigid wall using the two models. In practice, three types of contact forces can be observed during airbag inflation and subsequent contact with a solid object: the breakout forces which occur during the early stages of the inflation causing the rupture of the airbag cover, bagslap forces corresponding to contact between an unfolding bag and another object, and bag membrane forces which arise when the bag is fully inflated and in contact with another object. The simulation of the breakout forces in the folded airbag was beyond the scope of this study.

The setup was identical to the one in Reference [13]. It consisted of a rigid wall at a distance of about 15 cm (5.75 inches) from the base of the airbag. The airbag with the same folding pattern as in the previous section was used in this simulation. Inflated airbag configurations at 15 msec and 50 msec from the postprocessor LS-TAURUS are shown in Figures 8 and 9. Comparative results for computed volume, pressure, gas temperature, mass of gas and the contact forces are shown in Figures 10-14. As before, all the curves exhibited similar trends during the gas generation phase after which there was close agreement until the end of simulation. Observation of the z-force on the rigid wall shown in Figure 14 revealed that until 10 milliseconds the airbag was still unfolding and had not yet made contact with the plate. Therefore the contact force was zero. After this duration, the bagslap phenomenon could be observed when the unfolding airbag began to make contact with the rigid wall. During the period of 12 - 20 milliseconds, a constant force distributed over the area of contact was acting on the rigid wall. For the same period the results from [13] indicated a higher bag slap force of 2000N as compared to 800 N in the present study.

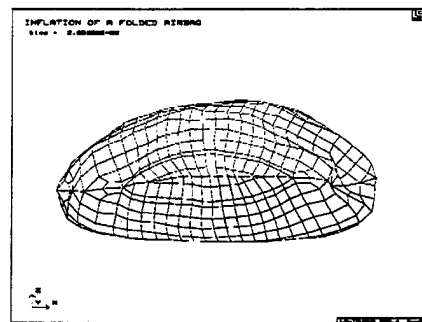
Between 20 - 23 milliseconds, the impact force sharply drops as the unfolding bag moved along the wall. This phenomenon lasted longer for the compared simulation lasting up to 30 milliseconds. In the present simulation, at the end of 30 milliseconds the contact forces reached a maximum value of 4000N. From 25 milliseconds onwards, the airbag oscillated between the base support and the rigid wall causing oscillatory rigid wall forces. After the gas generation stopped, the pressure in the bag decreased due to gas venting.



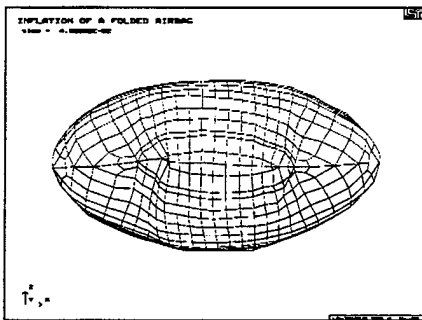
(a)



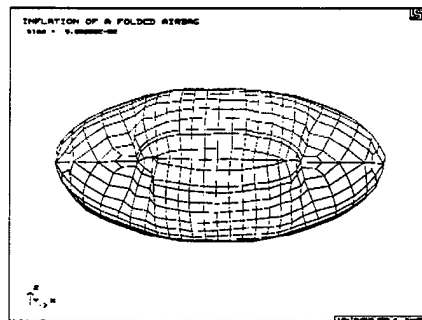
(b)



(c)



(d)



(e)

**Figure 2.** Inflation of a folded airbag in different stages: (a) oblique view before deployment, (b) side view at 15msec, (c) at 28msec, (d) at 45msec, and (e) at full inflation.

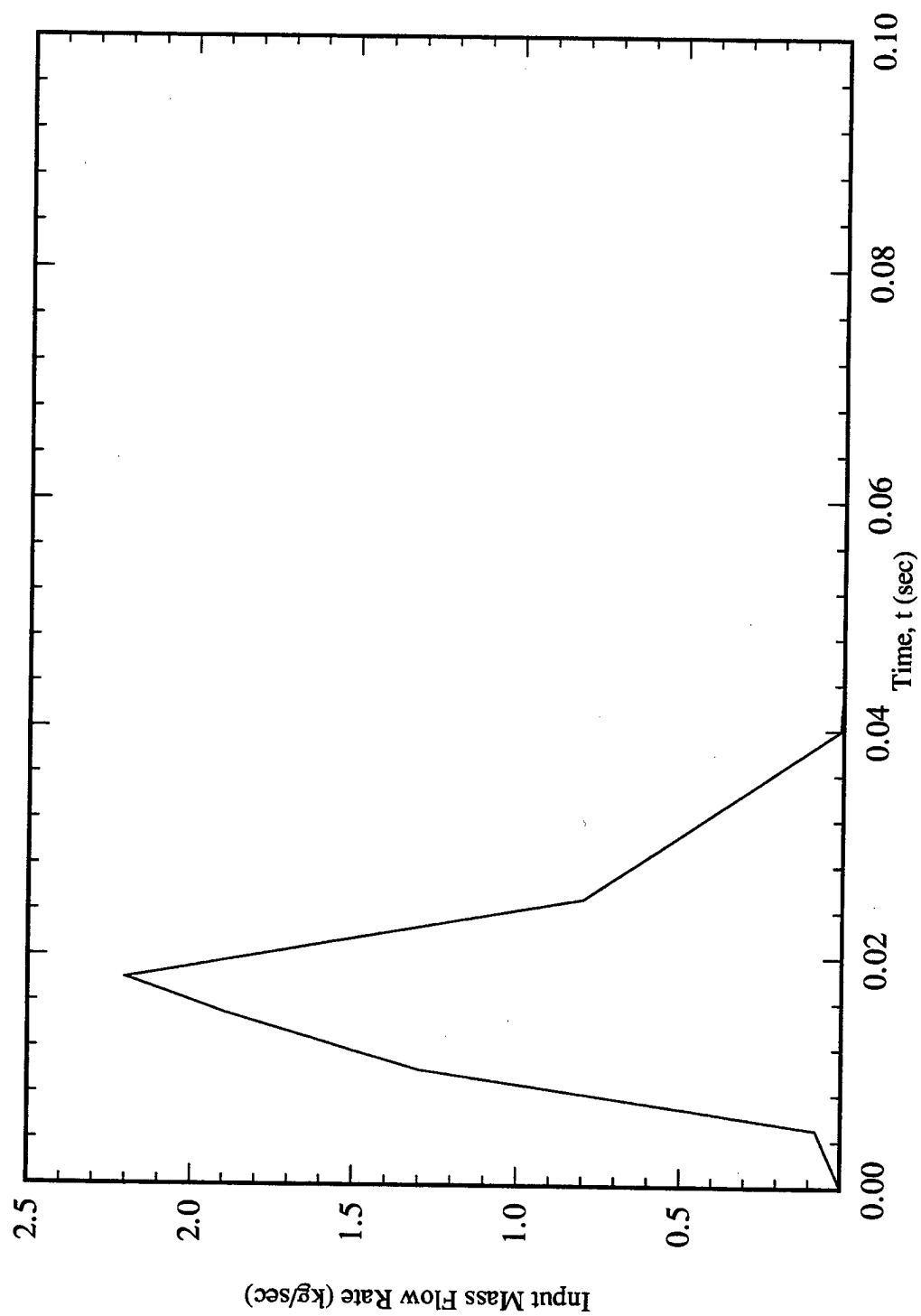


**Figure 3.** Load curve for the input mass flow rate.



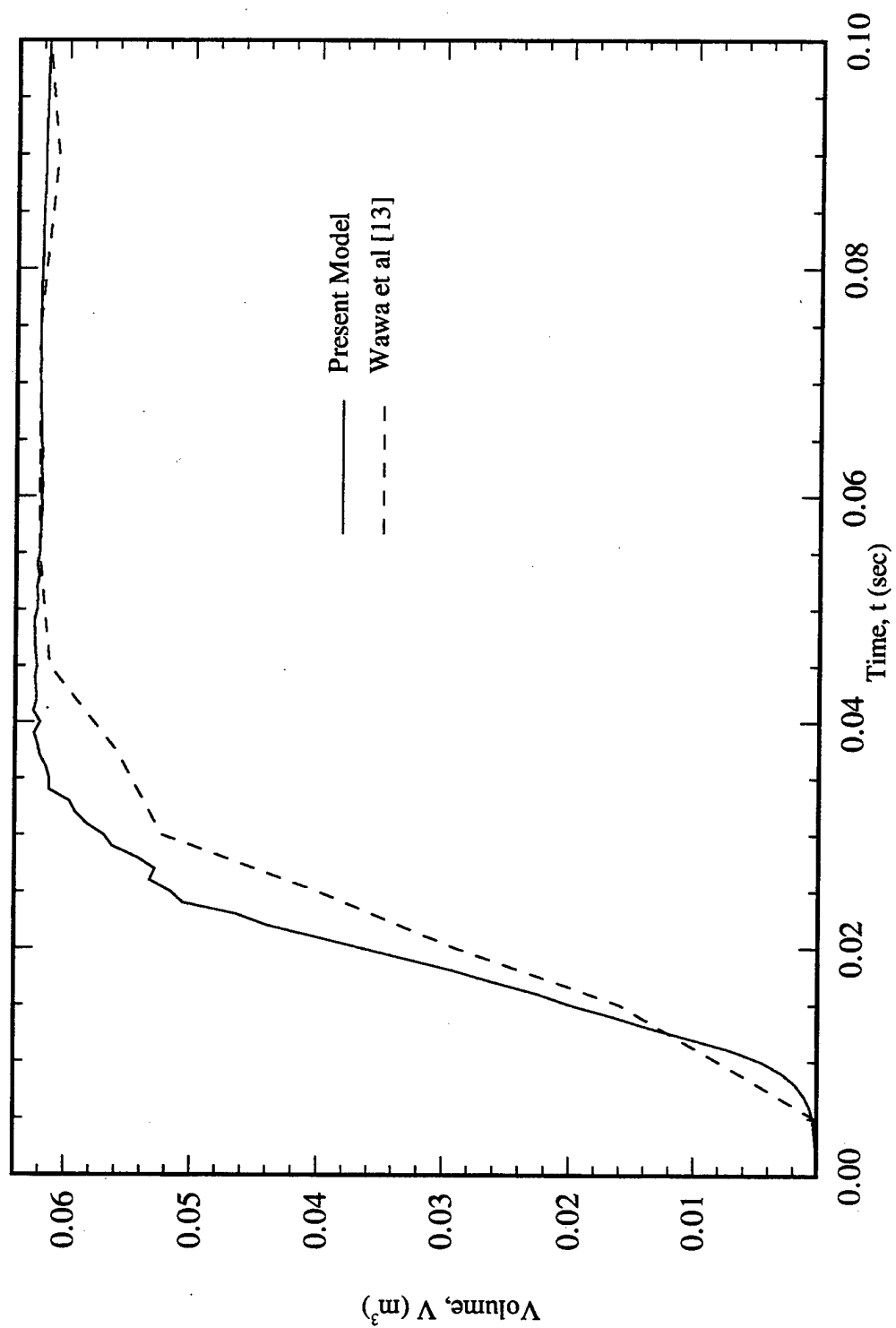


**Figure 4.** Time history comparison of the airbag volumes.

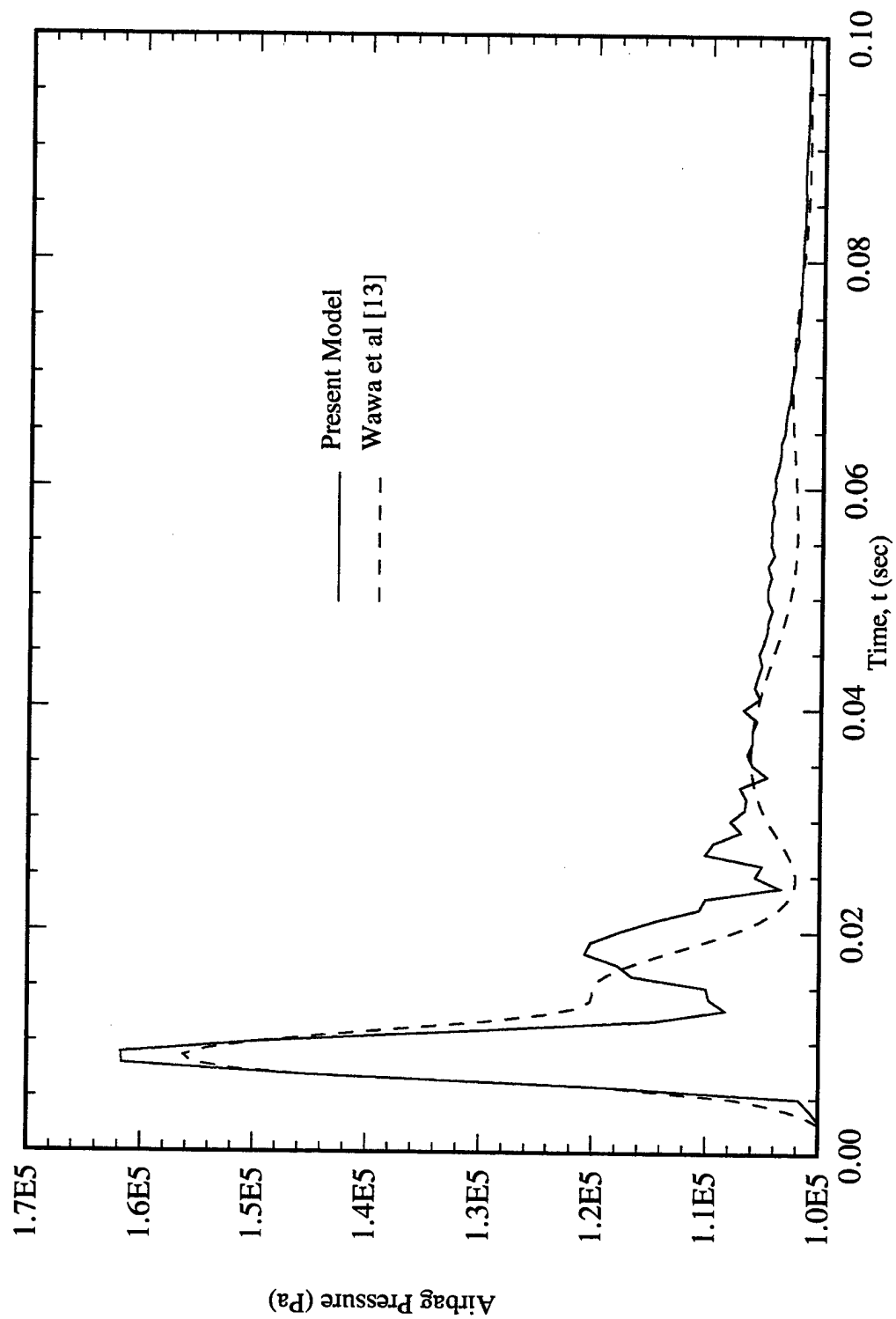


**Figure 5.** Time history comparison of the airbag pressures.

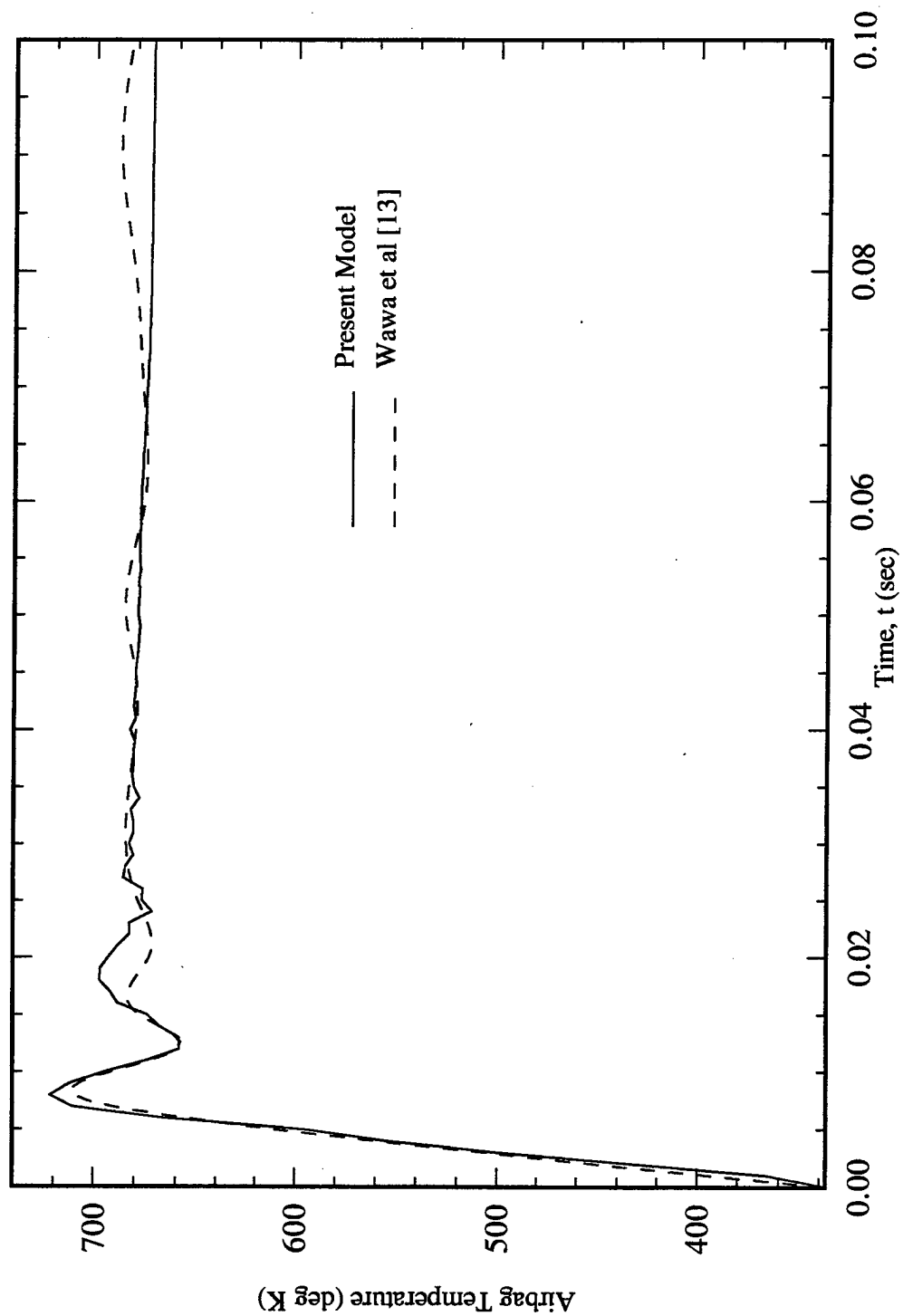


Figure 6. Time history comparison of the temperature within the airbag.

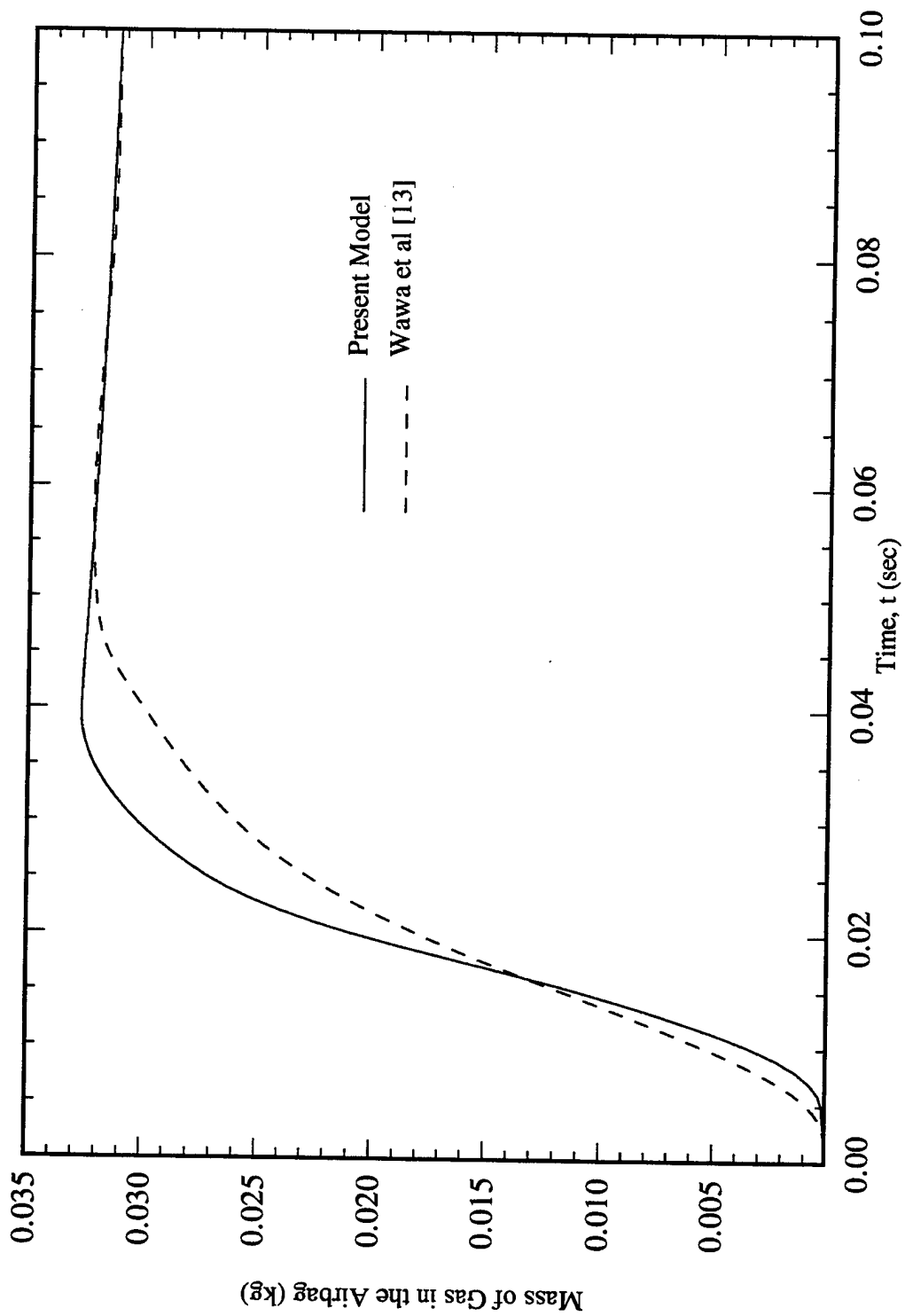
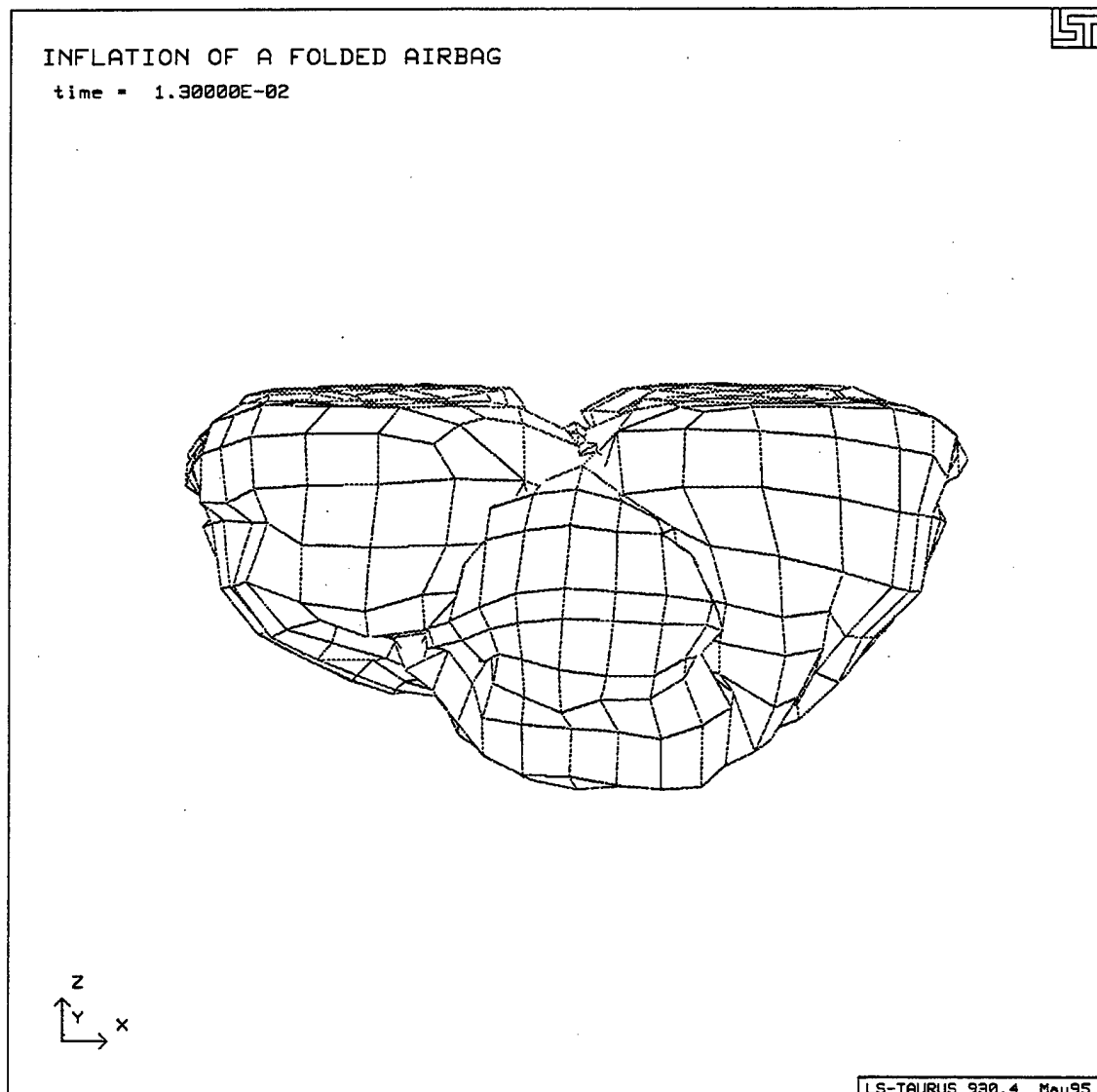
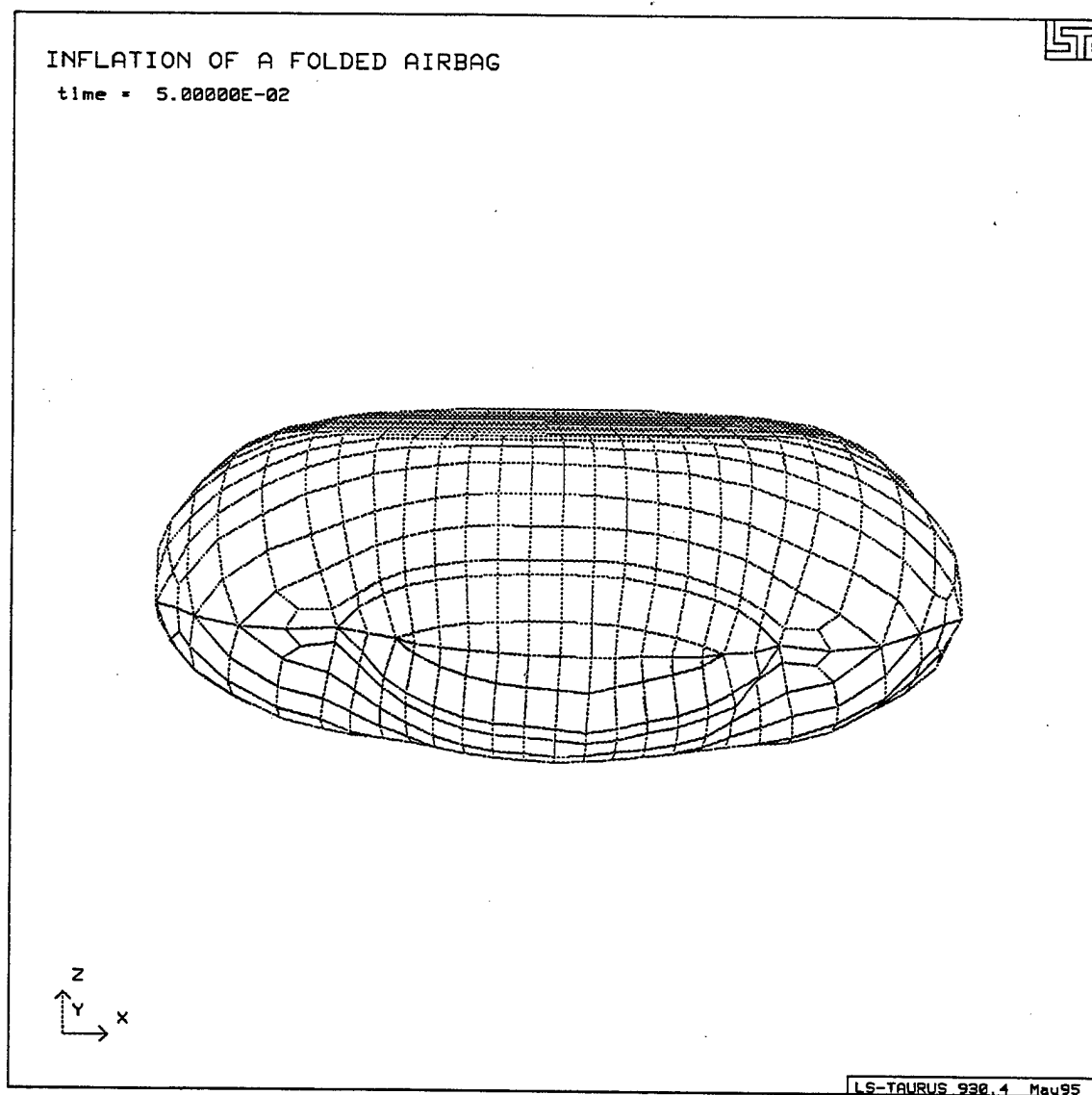


Figure 7. Time history comparison of the total mass of gas in the airbag during the period of simulation.



**Figure 8.** Side view of the inflating airbag at 15 msec colliding with the rigid wall.



**Figure 9.** Side view of the fully inflated airbag in contact with the rigid wall at 50 msec.

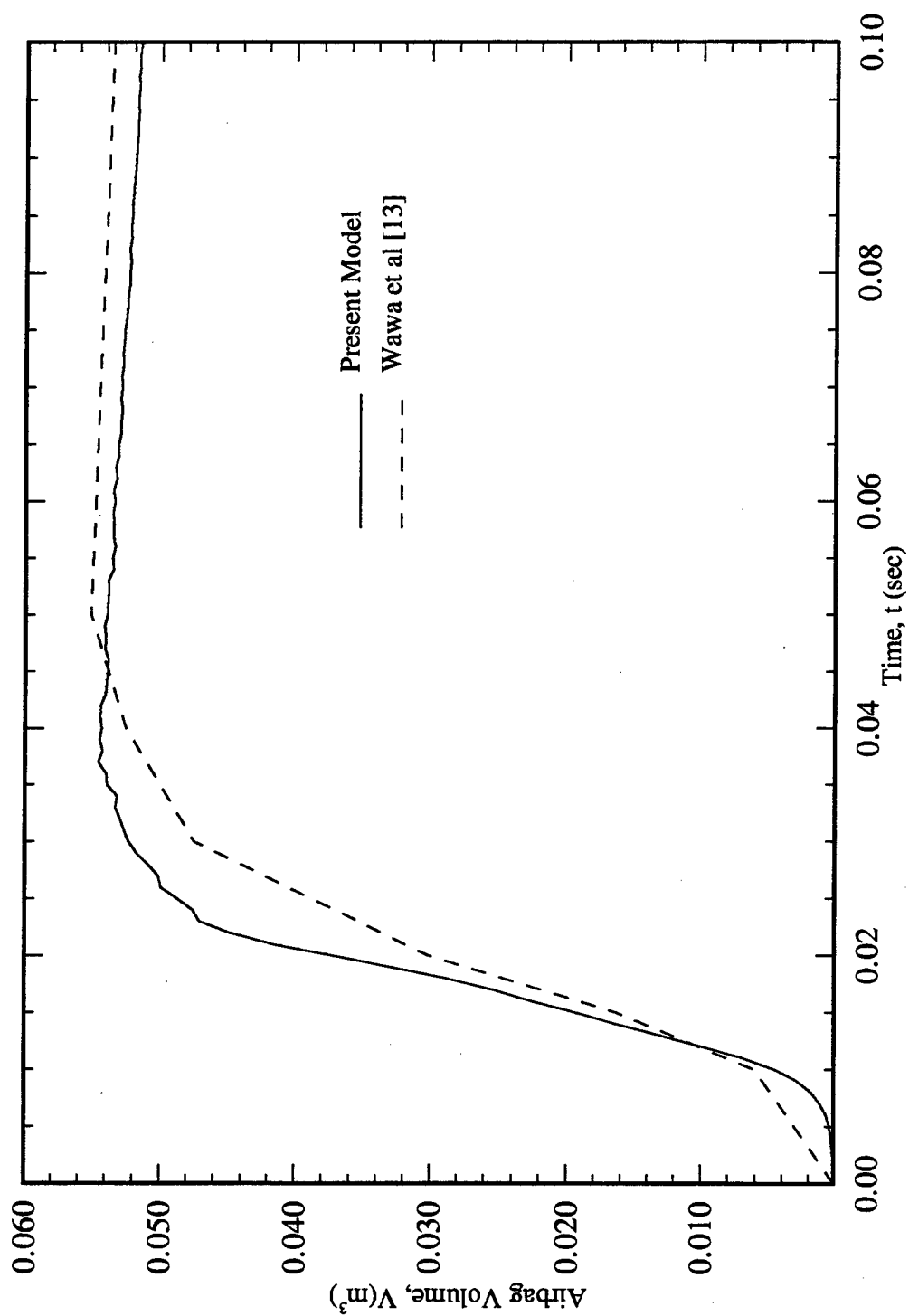


**Figure 10.** Comparison of airbag volumes for the simulation involving the rigid wall.

Comparison of pressure curves between the two simulations indicated peak pressures at around 10 milliseconds initially as seen in Figure 11. This pressure was similar to that in the airbag which was not subjected to impact with a rigid wall as shown in Figure 5. Again, the difference in the peak values of the pressure could be attributed to the difference in mass flow rate curves, though the trend remained similar. A second peak pressure at 15 milliseconds, corresponding to the bagslap phenomenon was observed. From 40 milliseconds onwards, both the curves dropped to ambient pressure in a similar fashion but the  $z$ -forces computed for the present simulation maintained a higher value throughout. After 40 milliseconds, the mass of gas in the airbag subjected to impact with the rigid wall was far less in comparison with the mass accumulated during pure inflation phase (discussed in section 1 above) as the higher pressure caused more gas flow out of the airbag. The two gas temperature curves for the present model and the reference model were in good agreement towards the end of the simulation as were the mass curves illustrated in Figures 12 and 13.

## B. PARAMETRIC STUDY

After gaining confidence in the validity of the airbag model using LS-DYNA3D software, a parametric study was conducted to analyze the effects of airbag parameters such as fabric density, bag elasticity, input gas temperature, and vent size on the impact between a rigid sphere and a deploying airbag. The rigid sphere was initially at a distance of 800 mm from the base support and was travelling with a velocity of 10 m/s. As a measure of the effect, the acceleration of the rigid sphere as influenced by the airbag inflation phase was studied. The initial finite element setup of the airbag and the sphere is depicted in Figure 15. The material properties of the airbag were the same as presented earlier in Table I. The collision of the spherical entity with the inflating airbag is illustrated in Figures 16- 19. Until 35 milliseconds, the airbag was inflated and sphere travelled with a constant velocity without any contact between the two. Between 35 and 40 milliseconds the sphere came in contact with the airbag. By 80 milliseconds the sphere had penetrated the airbag reducing its volume. At the end of the simulation which was 120 milliseconds, the sphere had rebounded and traveled away from the airbag. The accelerations of the sphere are in close agreement with the head accelerations from reference [14].



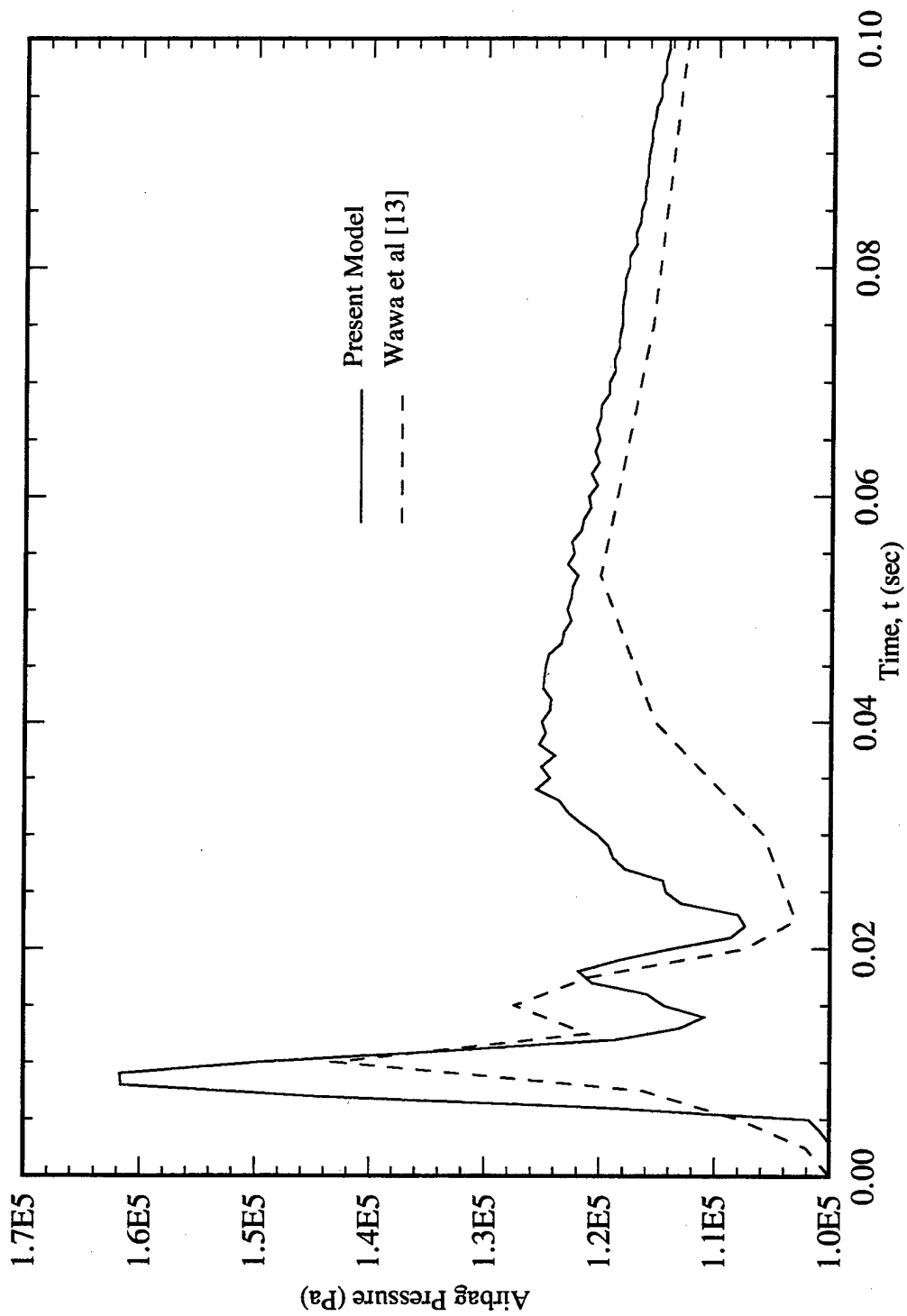


Figure 11. Comparison of airbag pressures for the simulation involving the rigid wall.

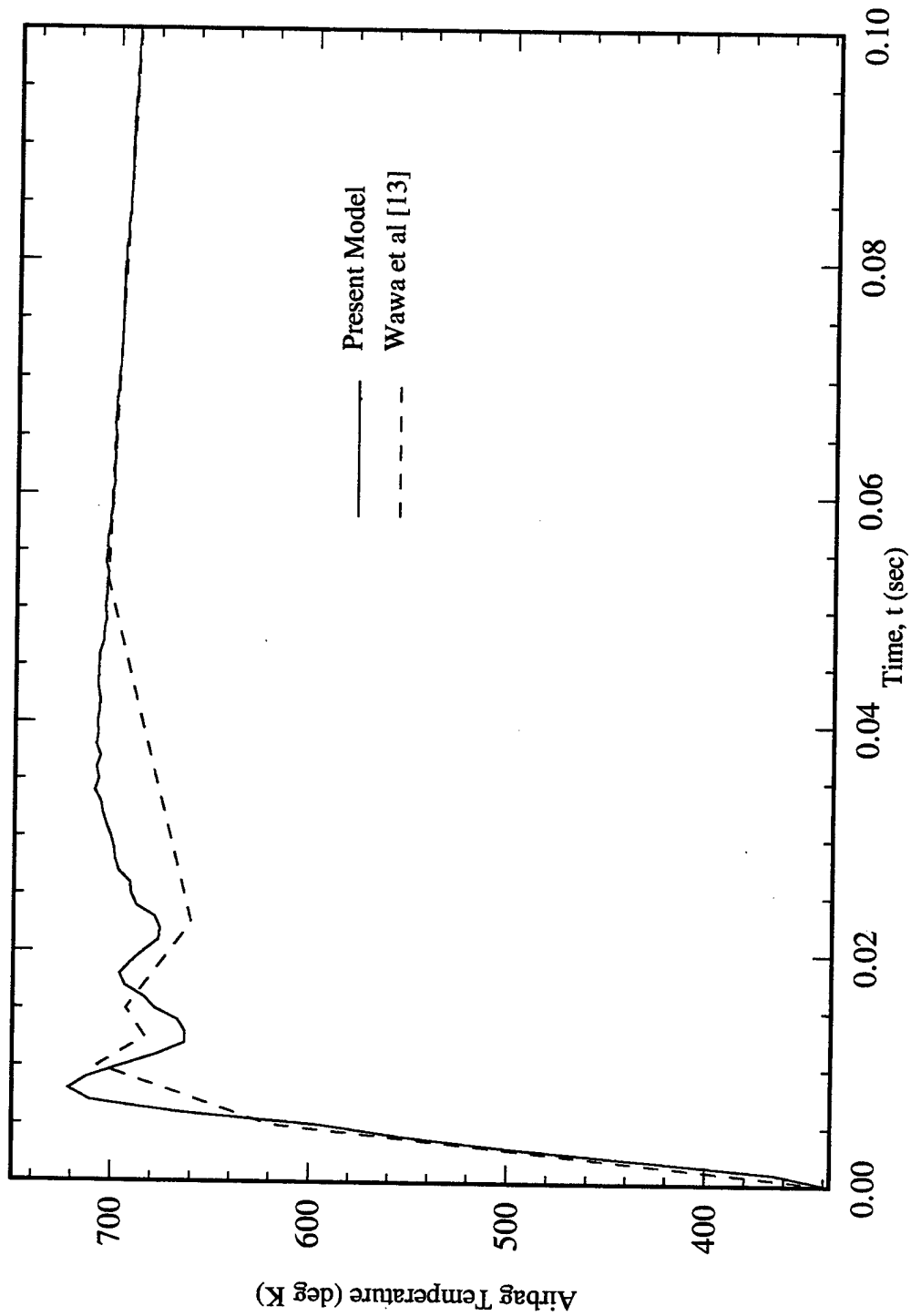
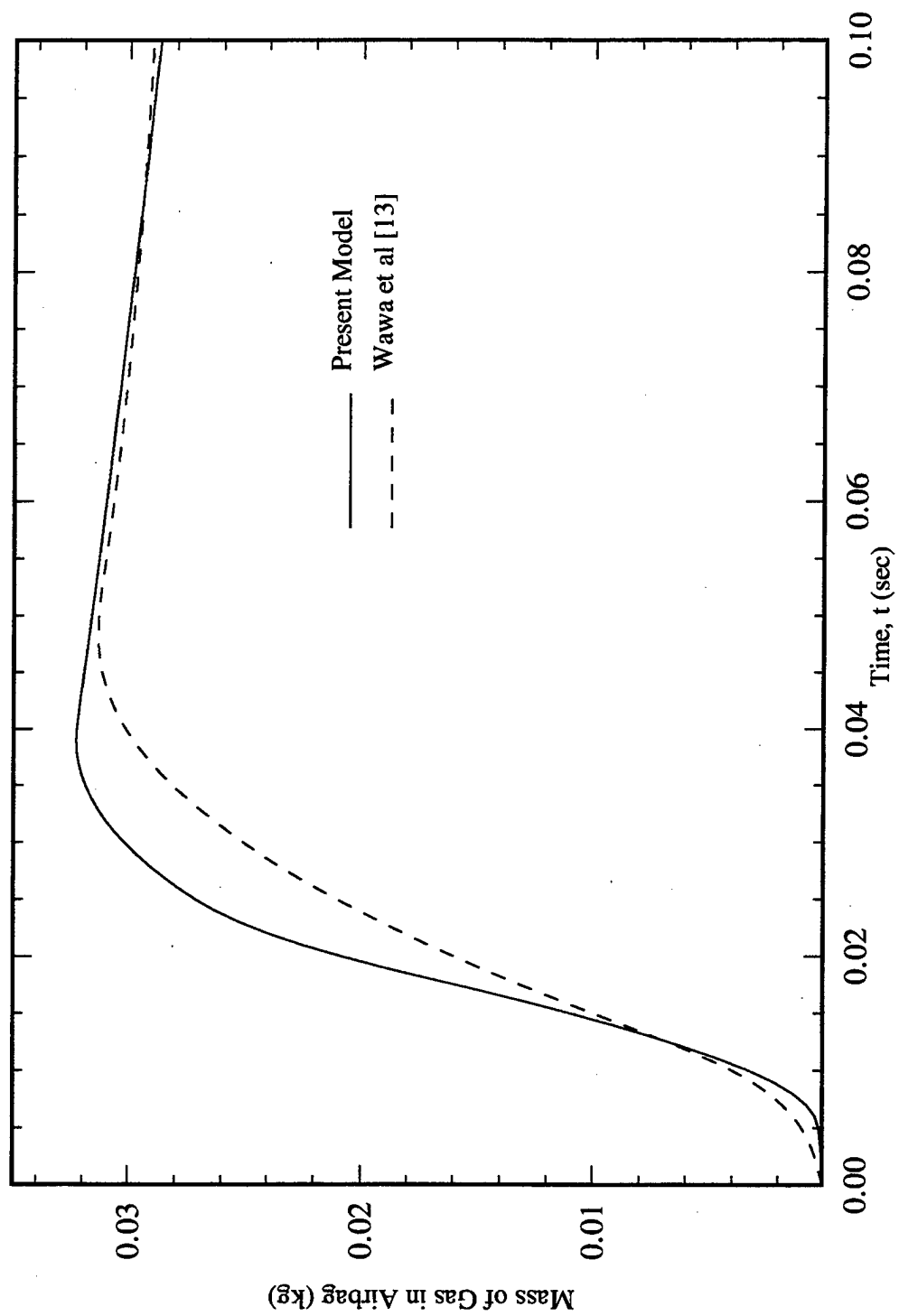


Figure 12. Comparison of airbag temperatures for the simulation involving the rigid wall.



**Figure 13.** Comparison of total mass of gas in the airbag for the simulation involving the rigid wall.

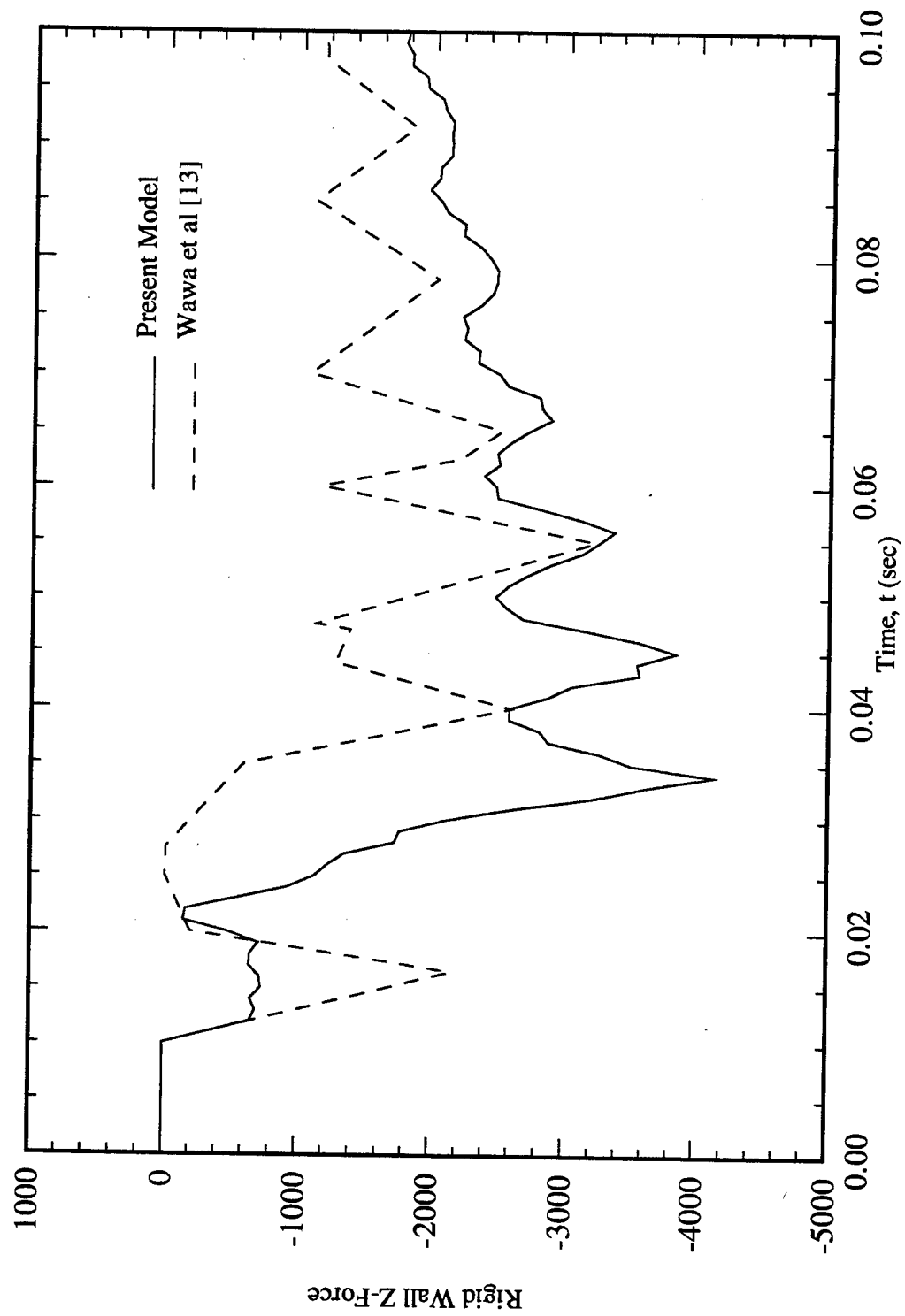
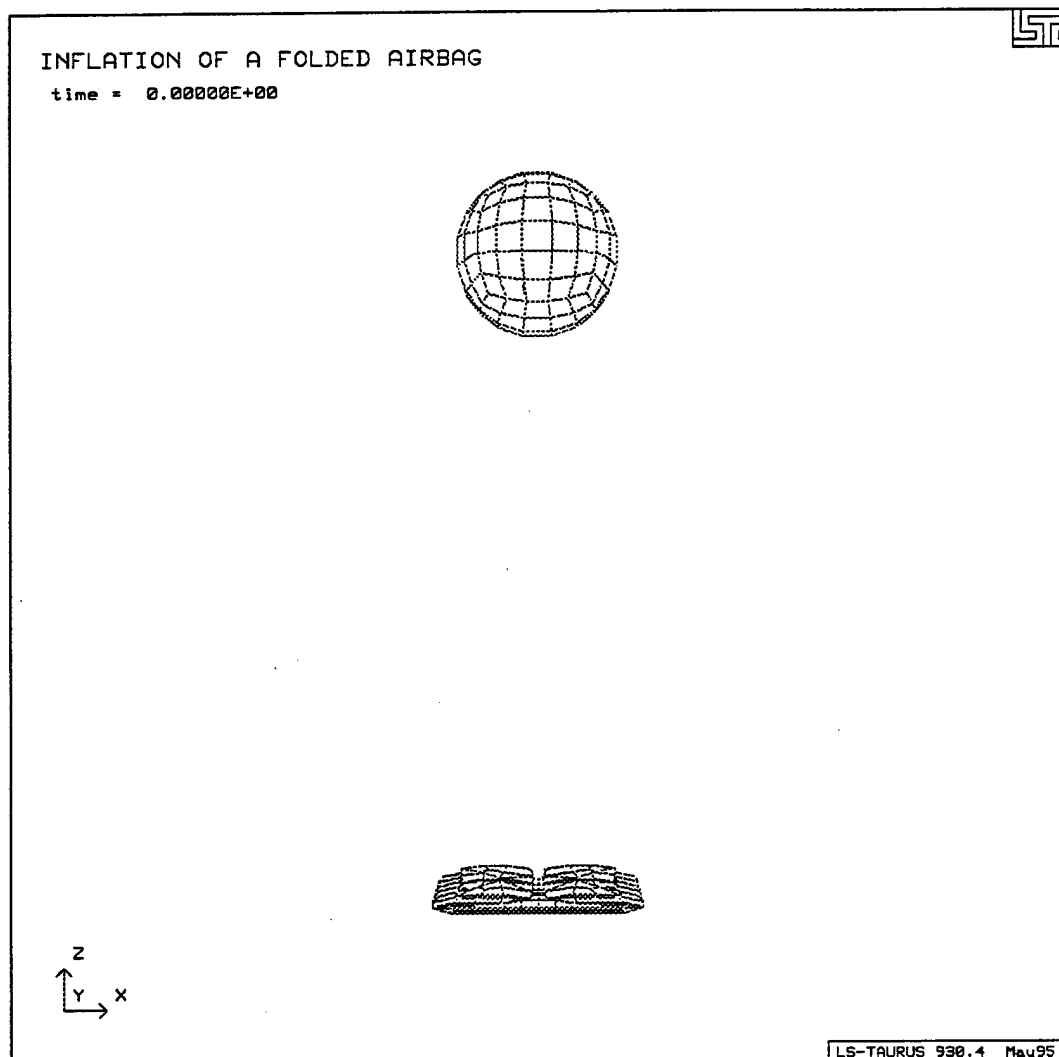
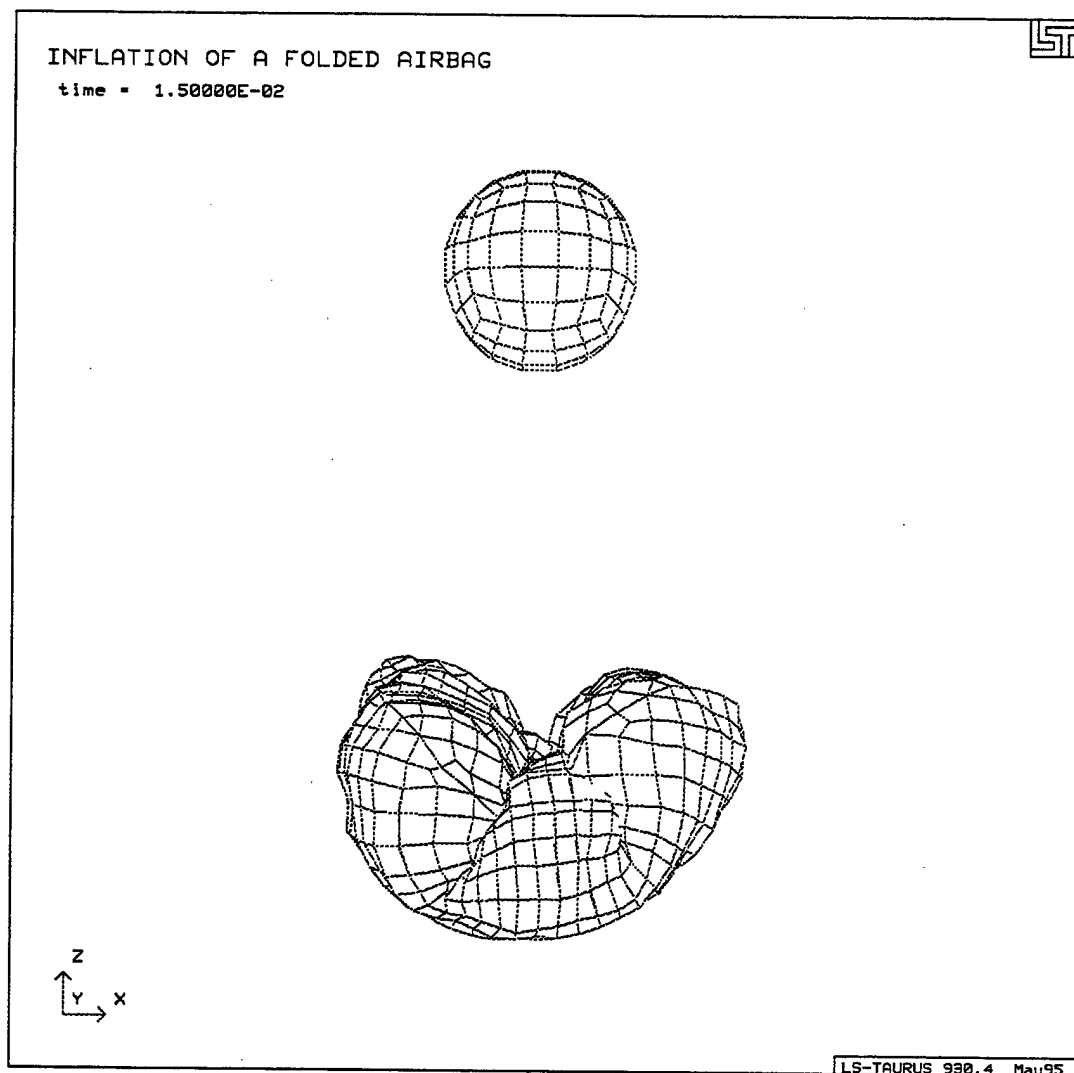


Figure 14. Comparison of rigid wall z - forces for the simulation involving the rigid wall.



**Figure 15.** Initial configuration of the folded airbag and the rigid spherical entity.



**Figure 16.** Side view of the unfolding airbag and sphere travelling with constant velocity at 15 msec.

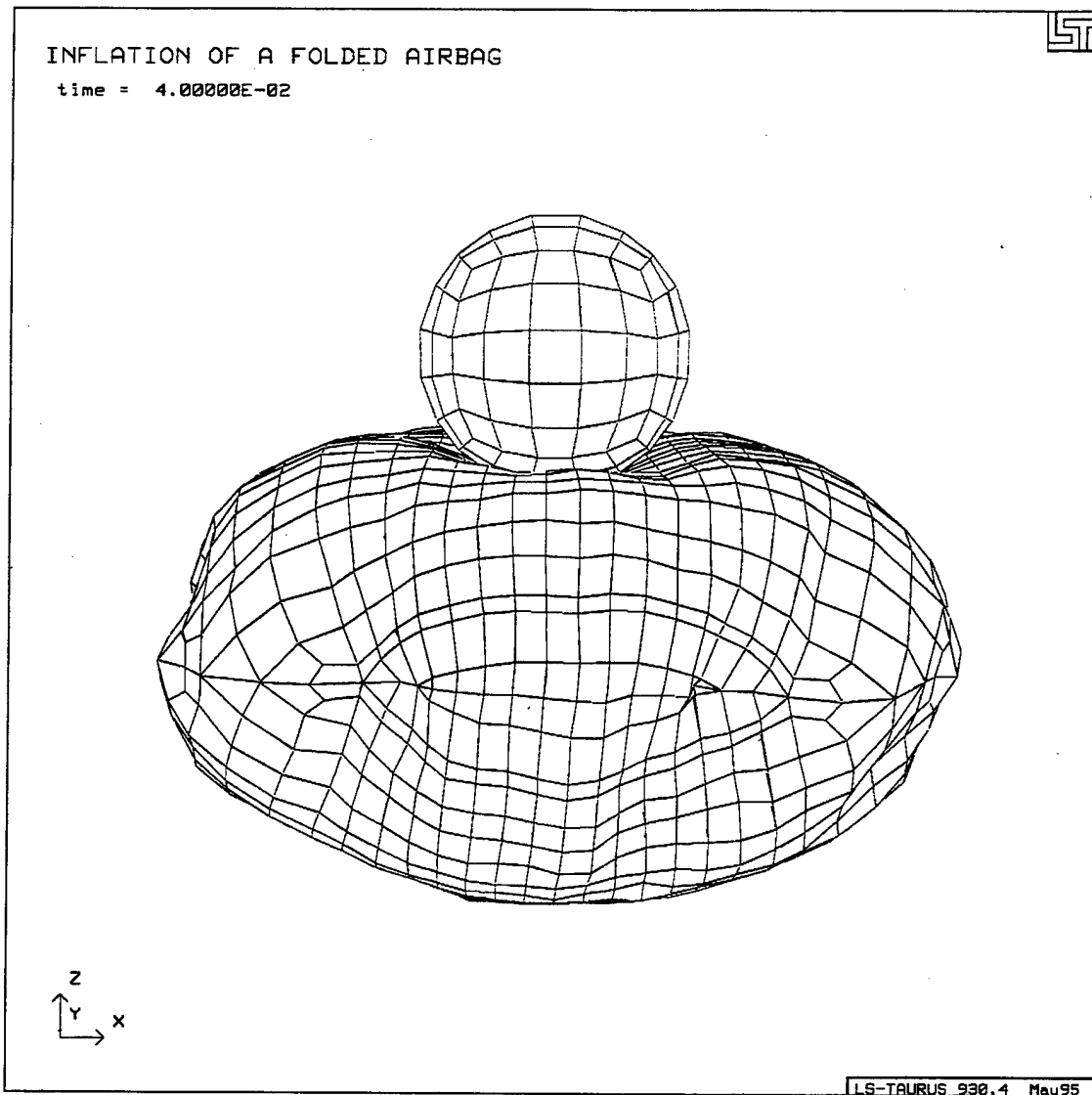


**Figure 17.** Side view of the inflating airbag in contact with the rigid sphere at 40 msec.

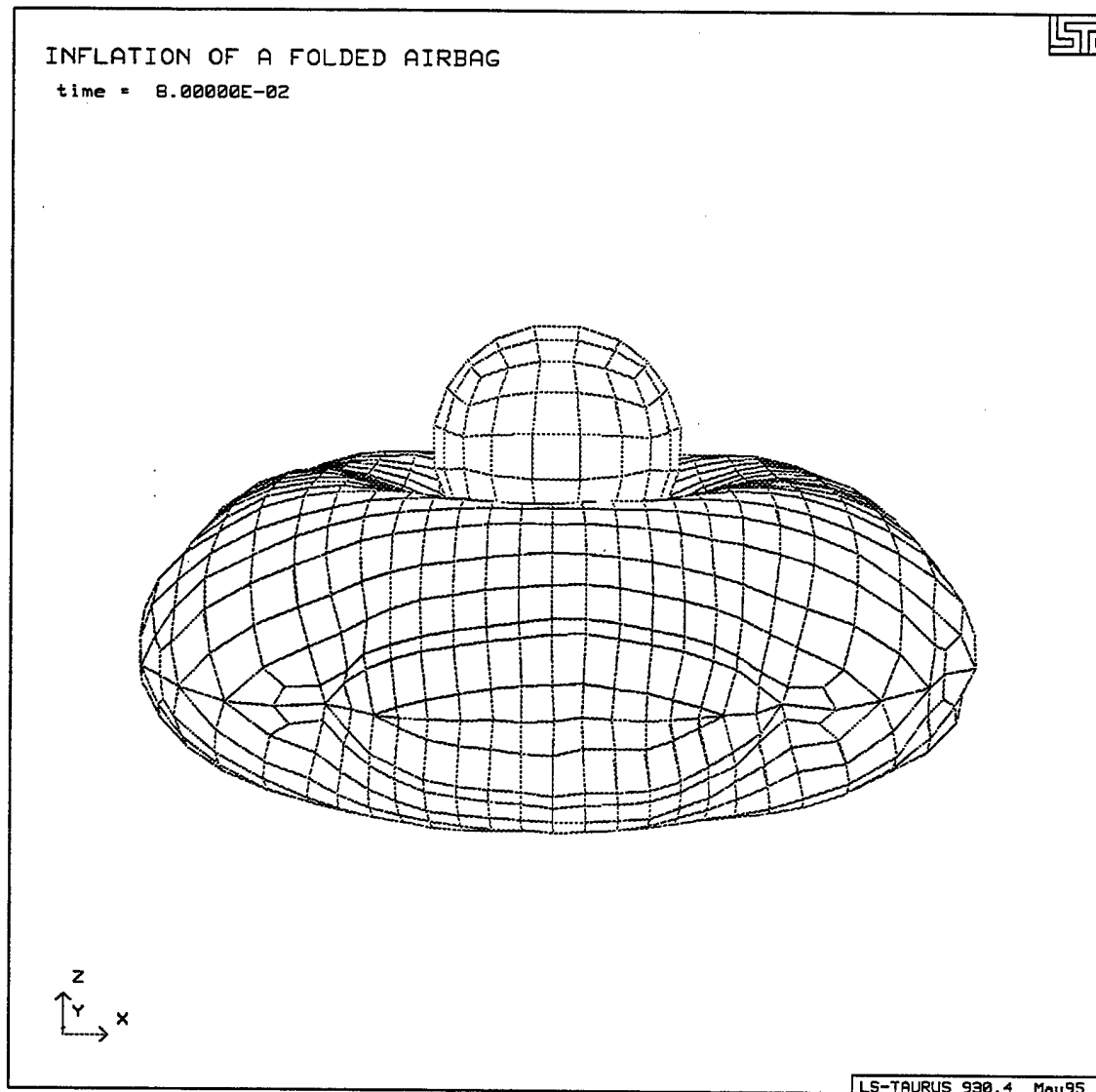


**Figure 18.** Side view of the rigid sphere penetrating the fully inflated airbag at 80 msec.



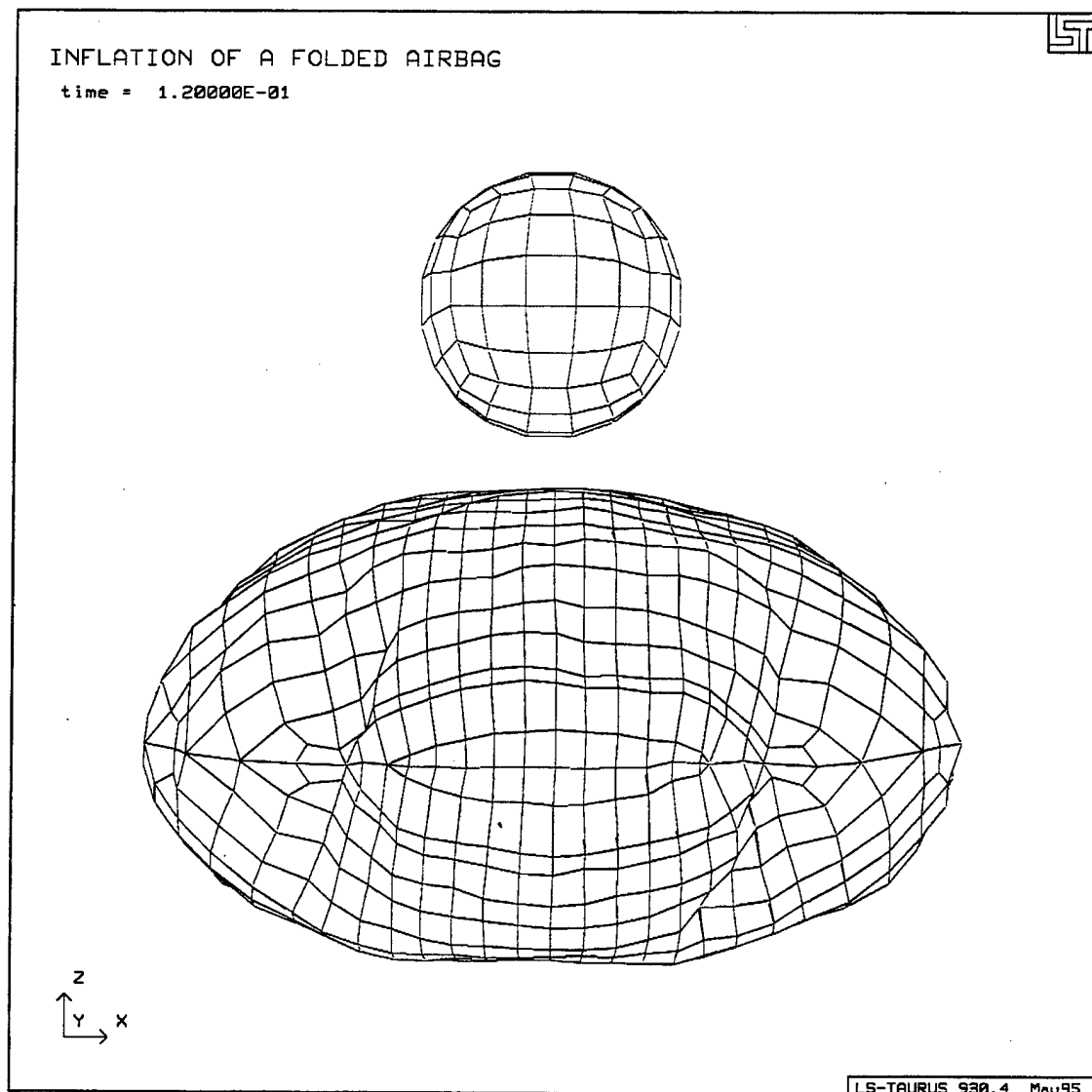


**Figure 19.** Side view of the rebounding sphere and airbag regaining shape at the end of simulation.

### 1. Effect of Fabric Density

To study the effect of fabric density on airbag deployment, a parametric study was carried out with airbags having fabric densities  $500 \text{ kg/m}^2$ ,  $1000 \text{ kg/m}^2$  and  $1500 \text{ kg/m}^2$ . Predictions of the resultant acceleration and z-velocity for the sphere are illustrated in Figure 20. The anticipated differences in times of initial contact by virtue of variations in material densities are indistinguishable in these figures for the three cases. However, the contact duration of 70 milliseconds remained the same for all the three cases. Peak accelerations ranging from 55 to 58 g's were observed for the sphere in all the simulations. The rebounding velocity of the sphere was highest for the fabric with lowest density which can be attributed to higher velocity of the airbag during unfolding and subsequent inflation as a consequence of low material density.

Figure 21 shows the volume and pressure histories. As expected, a higher bag volume and corresponding lower bag pressure were computed for the lowest bag density airbag model. The airbag volume was reduced during the contact phase, after which it began to regain its fully inflated shape. The pressure curves tended to converge once the gas generation stopped.

### 2. Effect of Bag Elasticity

Using the same material properties for the airbag but changing the bag elasticity, a parametric study was conducted to determine the dynamics of impact. Initial contact time was different for all the cases. For the fabric with  $1.3 \times 10^8 \text{ kg/m}^2$  elasticity, the acceleration was relatively higher compared to the other elasticity values used due to higher stiffness causing larger forces on the sphere. The larger contact time and higher rebound velocity of the sphere for  $0.5 \times 10^8 \text{ kg/m}^2$  elastic modulus value was attributed to greater bag stretch due to the lower elasticity. Rebound velocities computed were in the range of 7 to 8 m/sec in all cases as seen from Figure 22. The pressure curves in Figure 23 reveal marginally higher pressures for higher modulus of elasticity of the fabric. The softer (more compliant) material was found to cause larger bag volumes than a stiff material.

### 3. Effect of Input Gas Temperature

A parametric study was done on the effect of input gas temperature on the contact time and resulting acceleration of the rigid sphere. Figure 24 shows the accelerations and velocity time

histories for input gas temperatures ranging from 600 to 800 deg K in steps of 100 deg K. For the 800 deg K case, the initial contact time was the earliest followed by simulations for 700 deg K and 600 deg K. The rebounding velocity for the case of 600 deg K input gas temperature was found to be significantly lower. At the end of the simulation, the sphere was still in contact with the airbag.

The evolution of volume and pressure in the airbag at different temperatures illustrated in Figure 25 show that the lowest value of input gas temperature results in low bag volume. All the pressure - time histories followed the same trend until contact after which they varied. This variation was attributed to gas leakage through the vents in the airbag.

#### 4. Effect of Venting

Three cases were considered for studying the effect of venting on contact interaction. In the first case, no vent holes were defined and in the subsequent cases ventholes of areas 6.284 sq cm and 9.426 sq cm were considered. In all the simulations the coefficient of discharge of the venthole was assumed to be 0.7. The analysis of the velocity and accelerations from Figure 26 is instructive. The initial contact time which was at 35 milliseconds was found to be same for all the three cases as the mass of gas flowing out of the bag was negligible compared to the mass of the gas flowing into the bag until the input mass flow rate reached zero. After the gas generation stopped at around 40 milliseconds, the effect of venting could be seen. The resulting acceleration and z-velocity were the highest for the airbag model without venting and lowest for the model with the largest exit hole area.

The pressure and volume curves indicated in Figure 27 were identical until the flow of gas into the airbag stopped, after which they assumed different paths depending on the vent area.

### **CONCLUSIONS**

A Finite Element simulation of the deployment of an initially folded airbag was carried out using the nonlinear three dimensional finite element program LS-DYNA3D.

In the first phase, the finite element airbag model implementation was verified and a comparison of the unfolding process and airbag parameters with previously reported simulation results showed good comparison. The small discrepancies were attributed to the difference in load curves used for the two simulations.

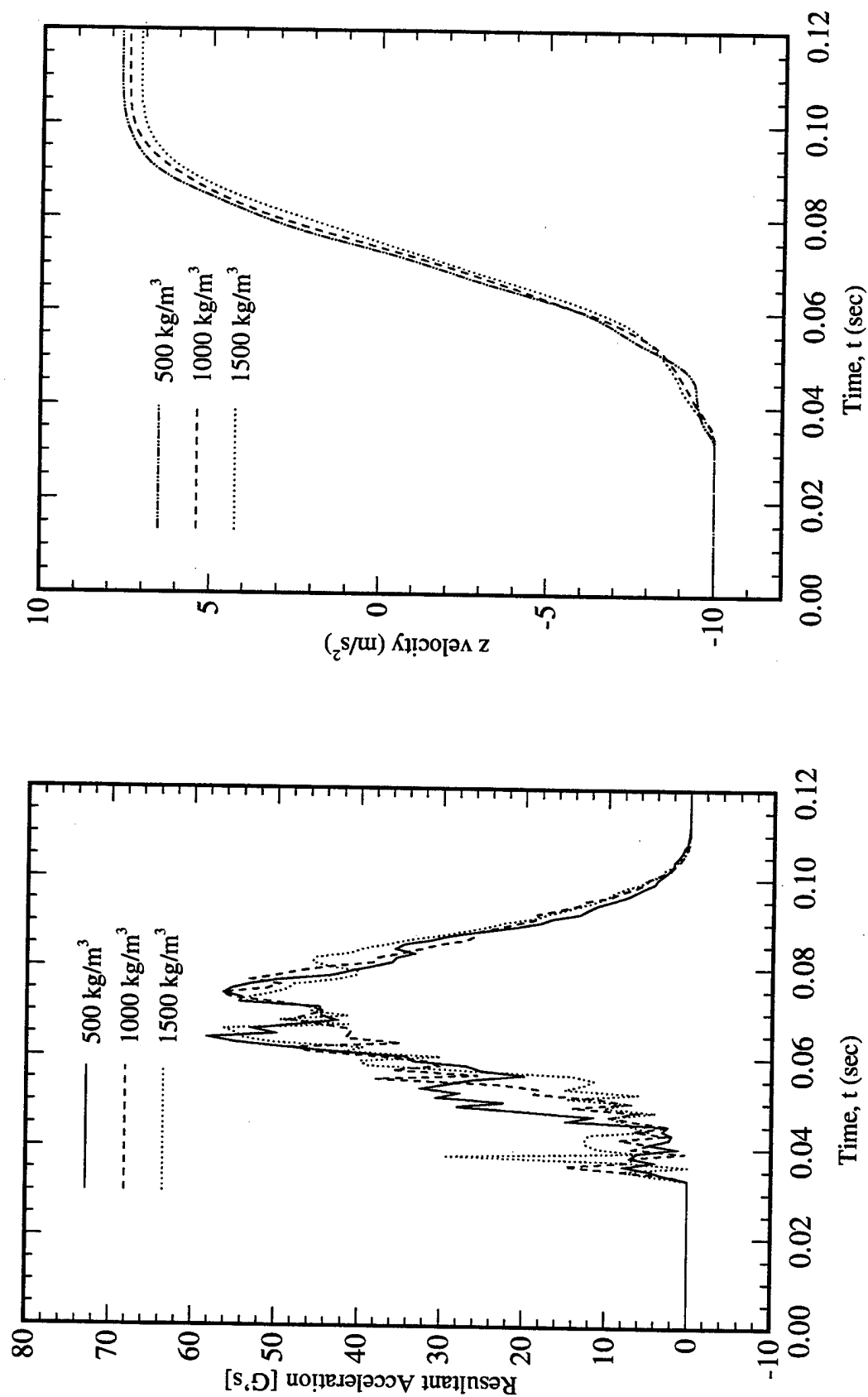


**Figure 20.** Resultant acceleration and velocity time histories of the rebounding sphere for various fabric densities.

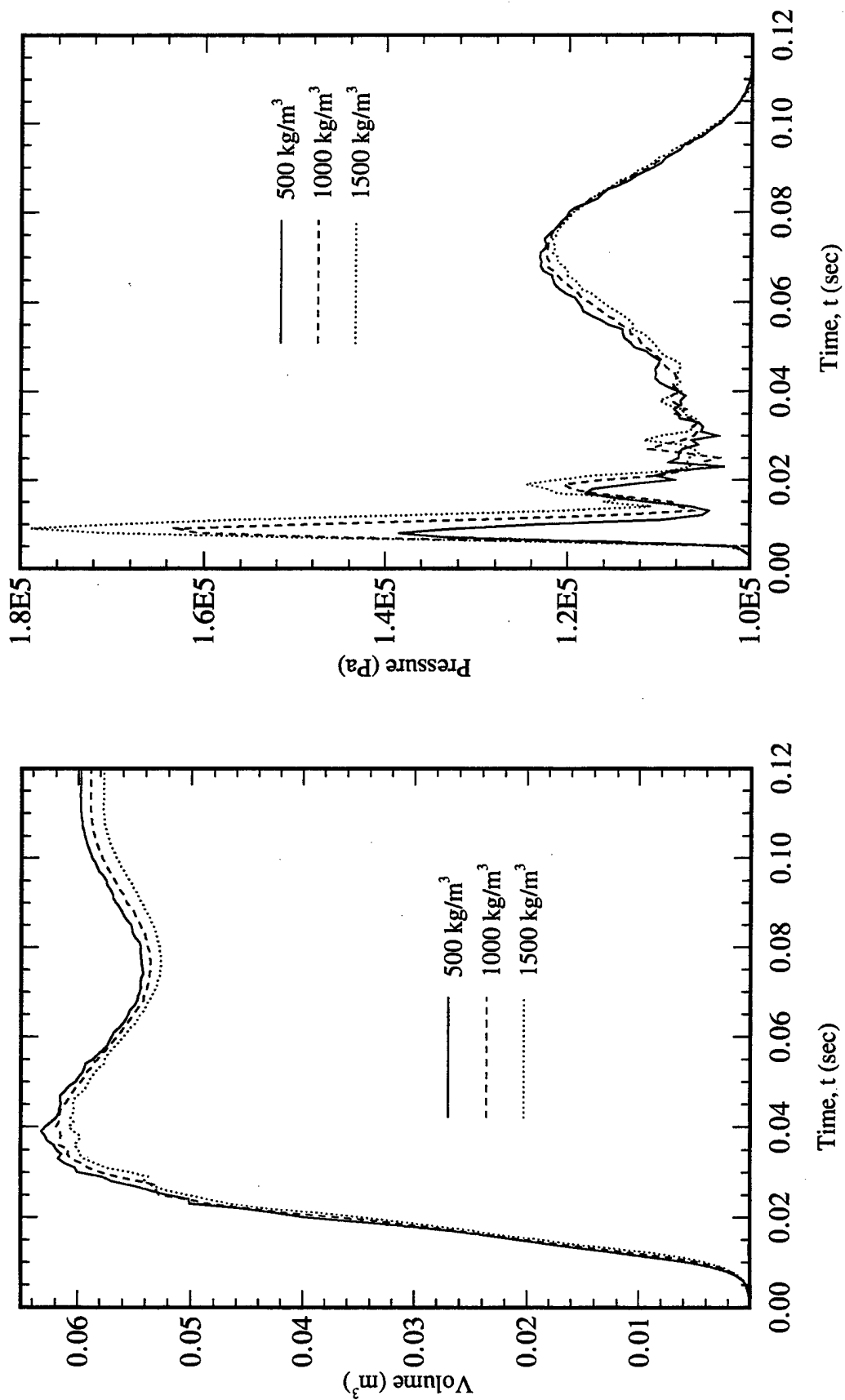


**Figure 21.** Volume and pressure curves for the airbag for various fabric densities.

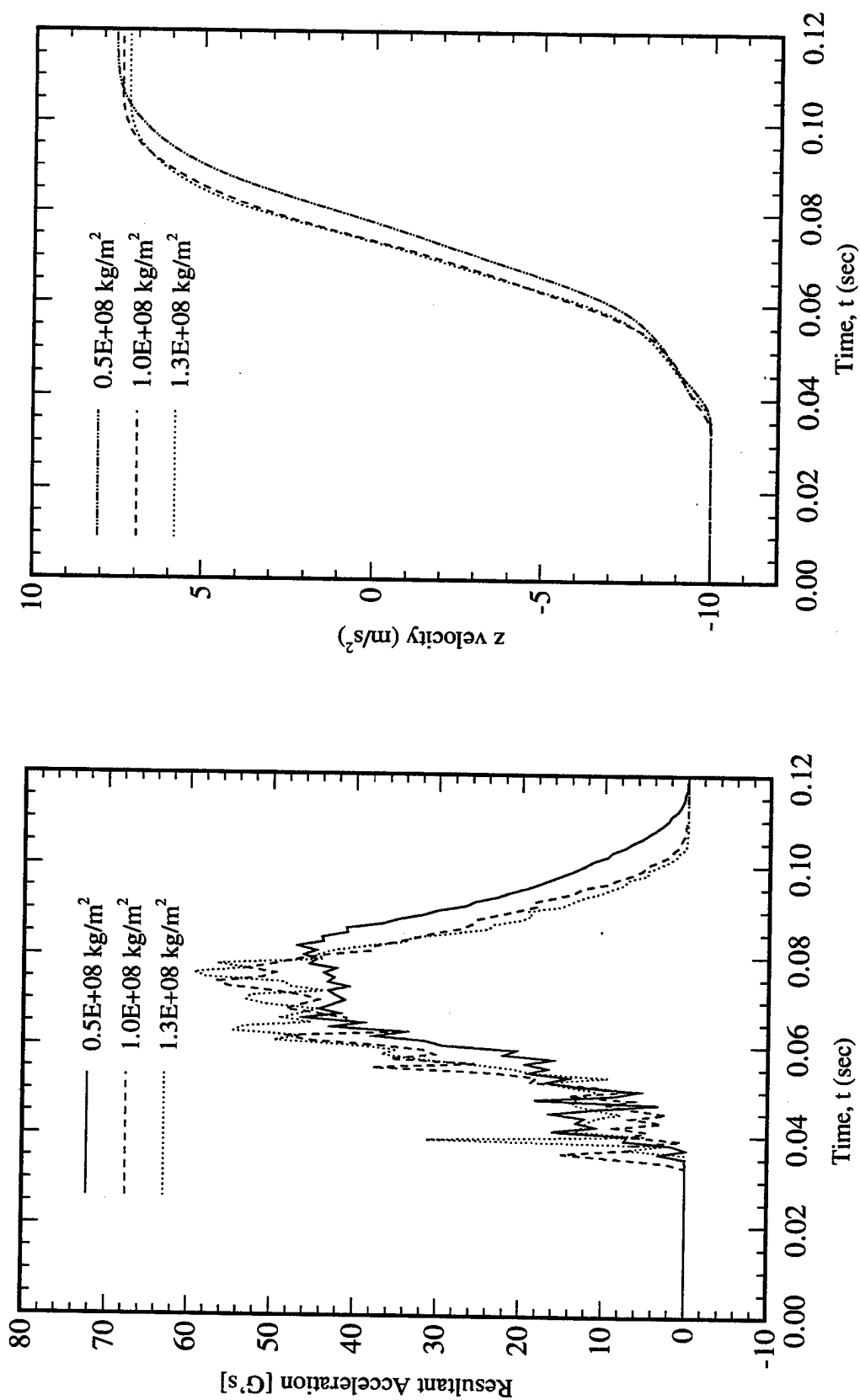


**Figure 22.** Resultant acceleration and velocity time histories of the rigid sphere for different values of bag elasticity.

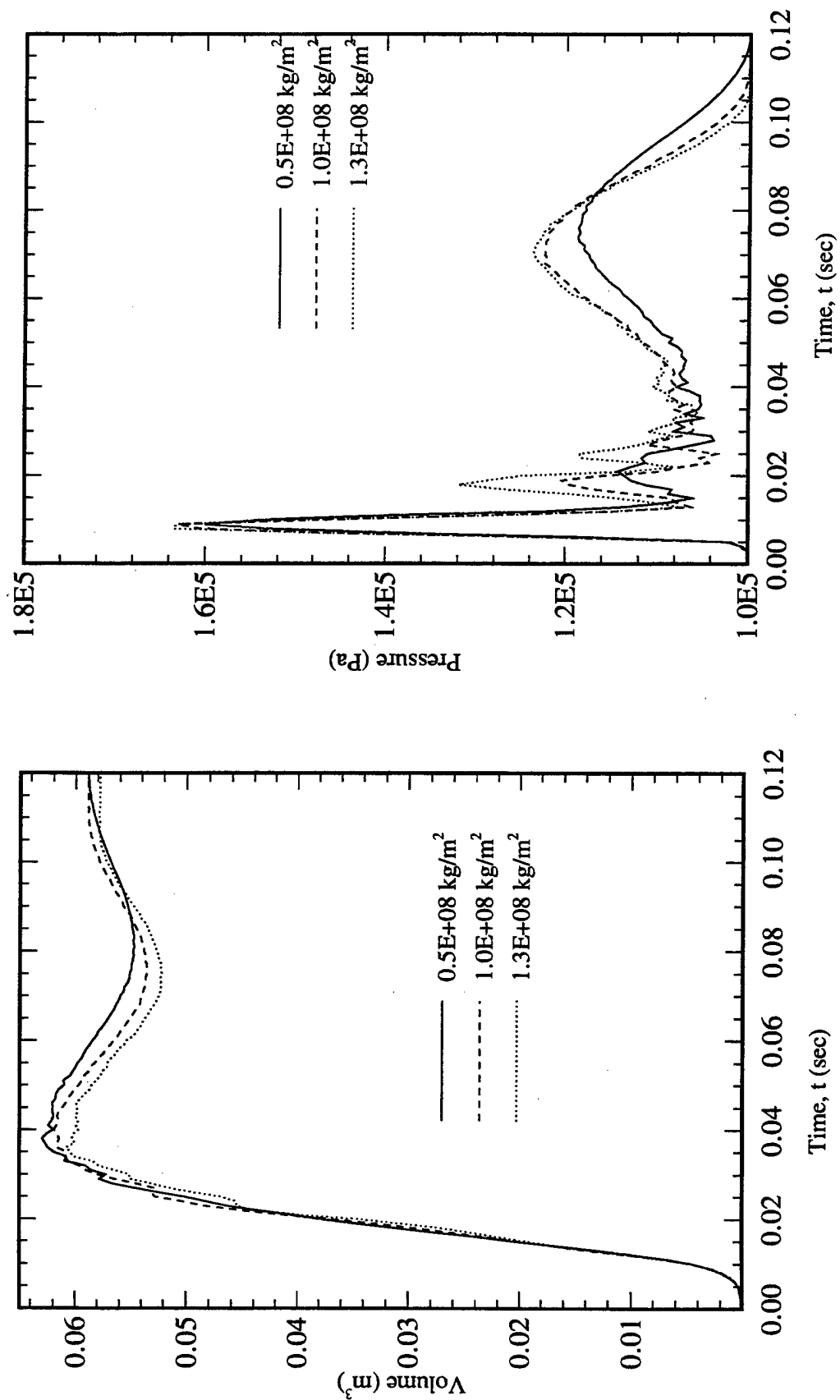
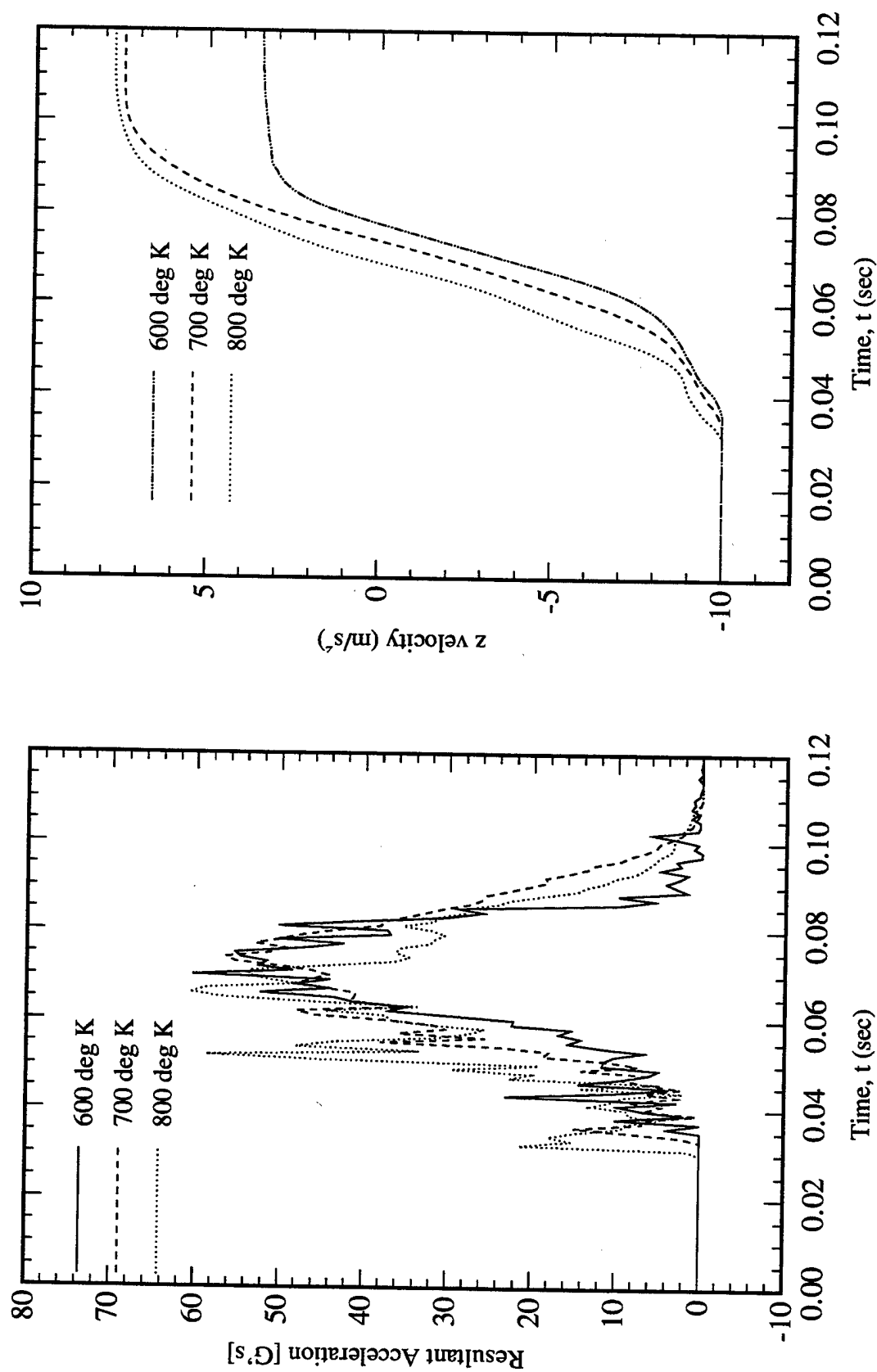


Figure 23. Volume and pressure time histories for the airbag for different values of bag elasticity.



**Figure 24.** Time histories of the resultant acceleration and velocity of the rigid sphere for a parametric variation of the input gas temperature.



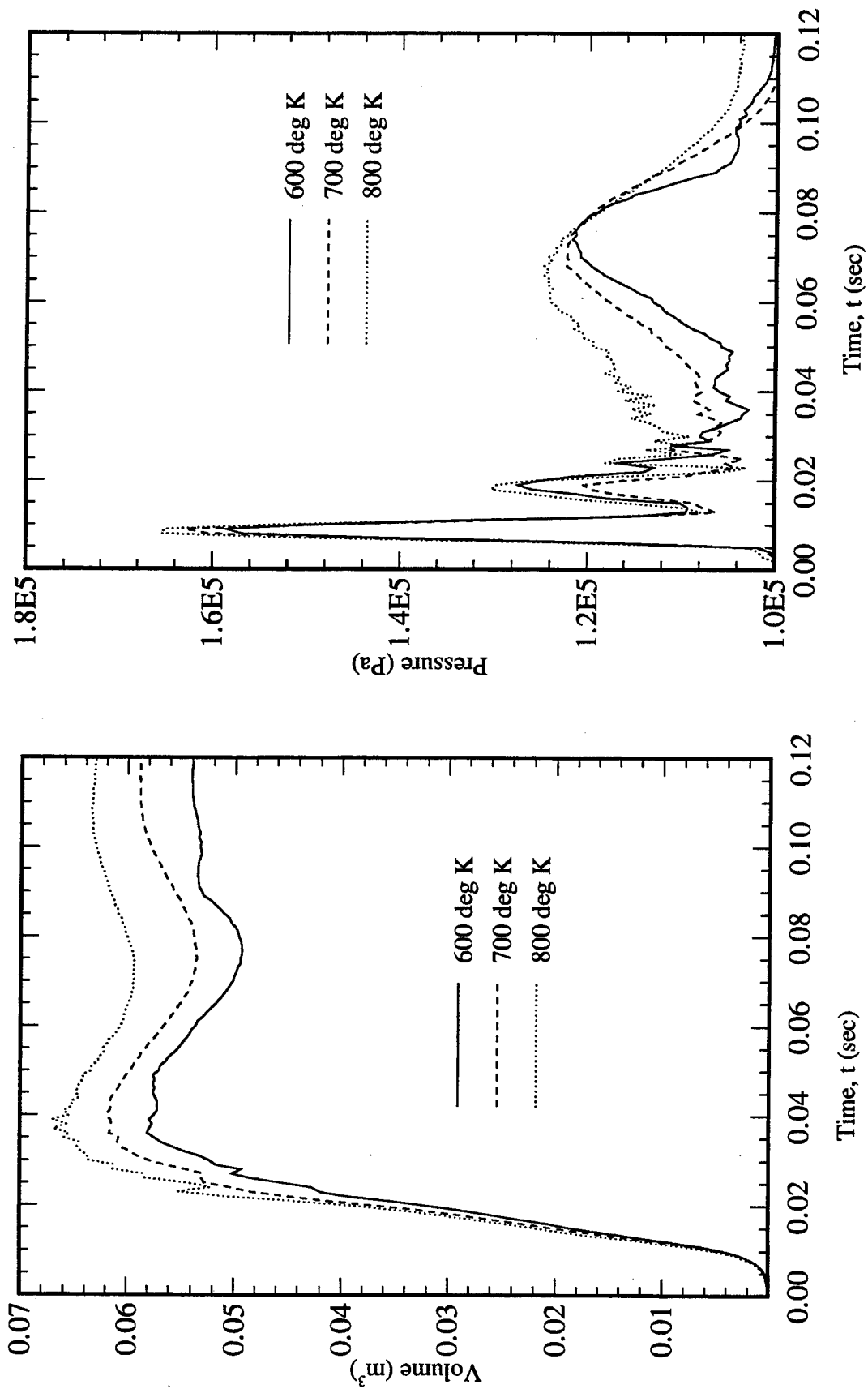
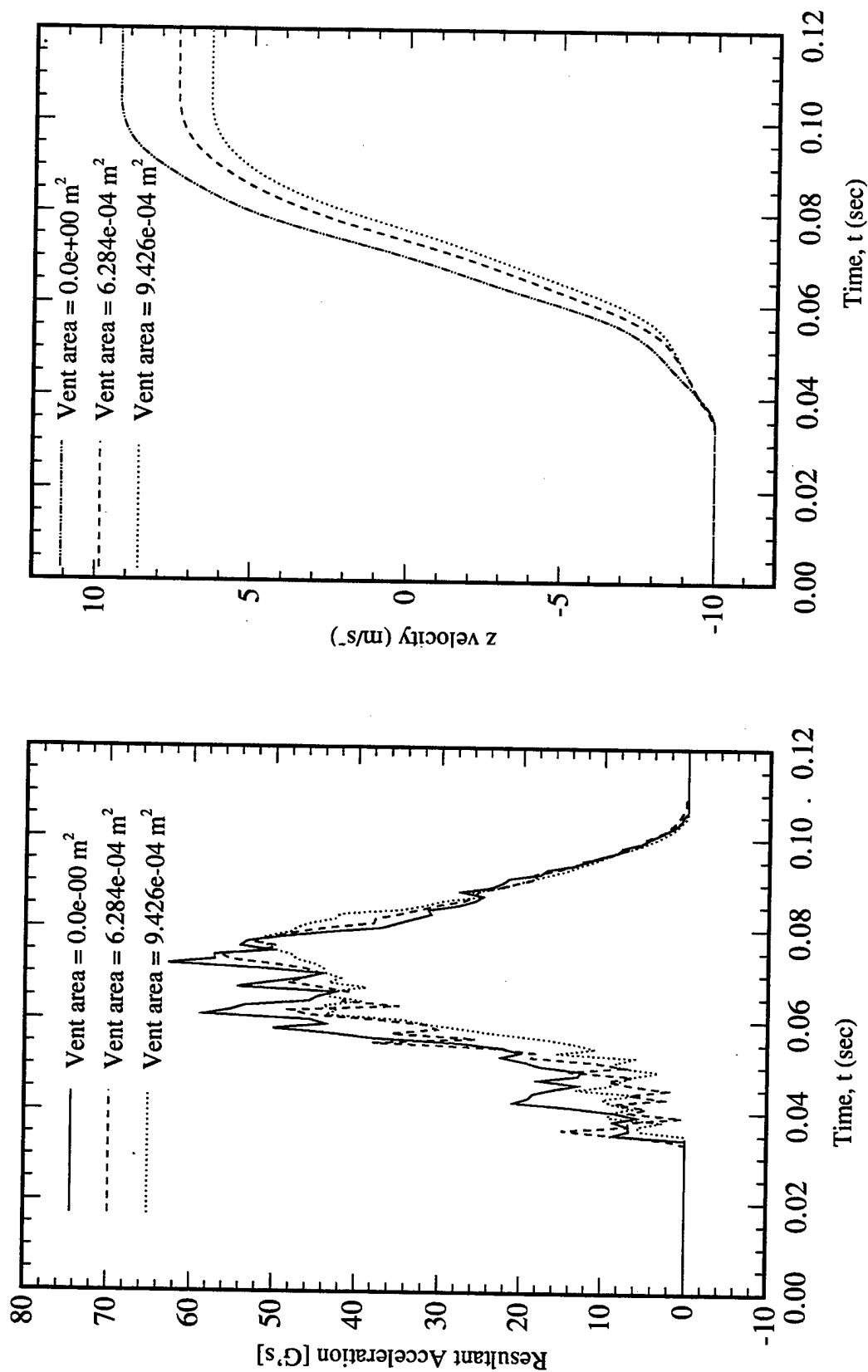
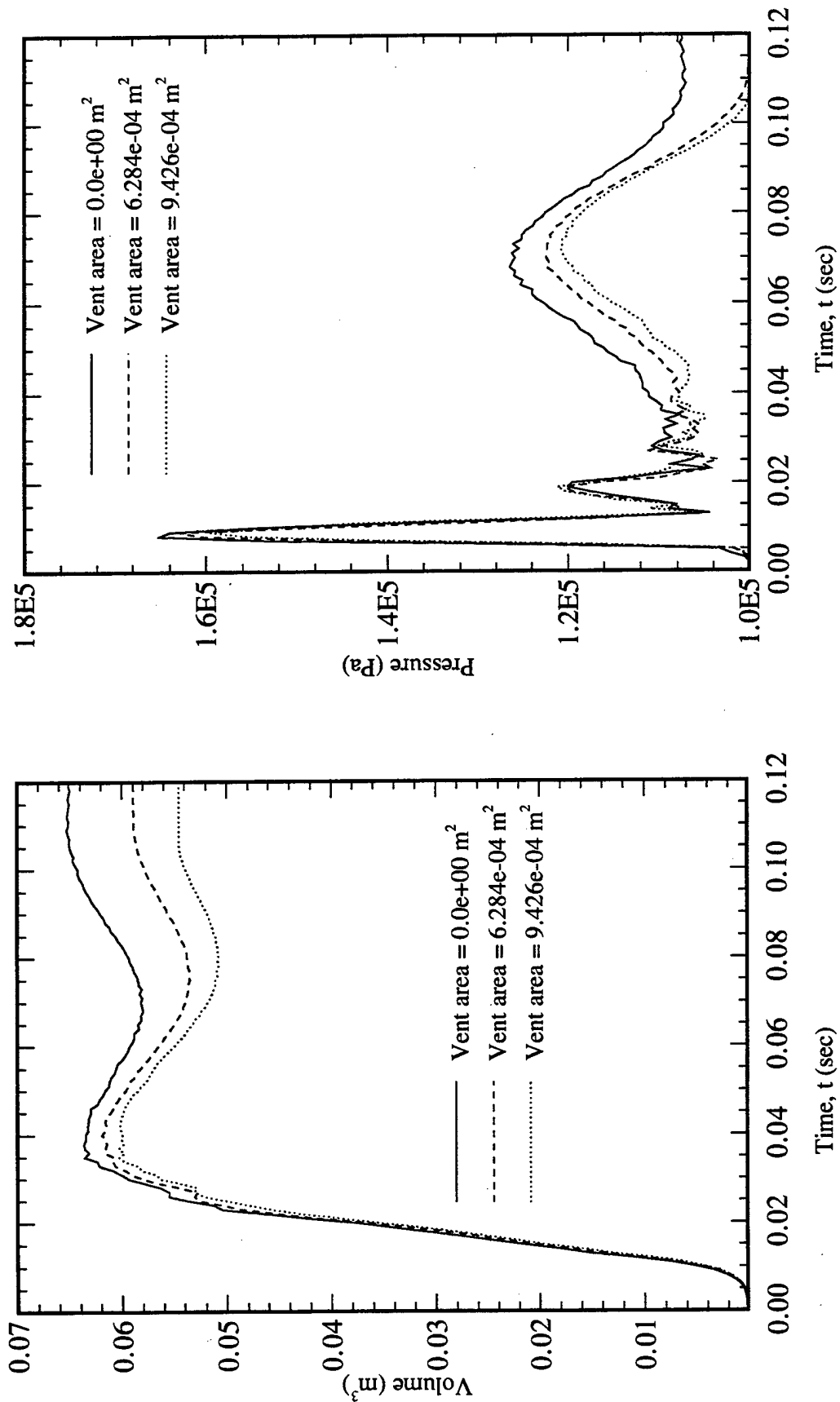


Figure 25. Time histories of the volume and pressure of the airbag for a parametric variation of the input gas temperature.



**Figure 26.** Time histories of the effect of airbag venting on resultant acceleration and velocity of the impacting sphere.



**Figure 27.** Time histories of the effect of airbag venting on volume and pressure of the airbag.

In the second phase, the deploying airbag model from the first phase was impacted against a rigid wall in order to capture the contact forces generated during the unfolding and subsequent contact with a rigid body. The airbag response characteristics, as well as the rigid wall forces were compared with results from a similar simulation to verify the finite element solution. The computed airbag characteristics such as volume, pressure, temperature and total mass time histories were in good agreement while the results for the contact forces were satisfactory.

In the final phase, a parametric study was conducted to investigate the influence of the airbag parameters on contact during collision of the airbag with a solid object. The airbag parameters considered were fabric density, bag elasticity, input gas temperature, and venting. It was inferred from the simulation that the fabric density did not have a significant effect on the resultant acceleration of the rebounding object while the bag elasticity had considerable effect on the acceleration of the solid object as well as on the contact duration. A low input gas temperature resulted in low bag volume and pressure. An increase in the vent area resulted in reduced acceleration for the impacting sphere. In an actual crash situation, the purpose of the airbag is to prevent injury and reduce the acceleration of the anatomical entity that may come in contact.

## REFERENCES

- [1] Viano, C. David, Effectiveness of Safety Belts and Airbags in Preventing Fatal Injury, SAE Paper No. 910901, 1991.
- [2] Digges, H. K., V. Roberts, J. Morris, Residual Injuries to Occupants Protected by Restraint Systems, SAE Paper No. 891974, 1989.
- [3] Wang, J. T., J. D. Nefske, A New CAL3D Airbag Inflation Model, SAE Paper No. 880654, 1988.
- [4] Nieboer, J. J., J. Wismans, P. J. A. De Co, Airbag Modelling Techniques, SAE Paper No. 902322, 1990.
- [5] Lakshminarayan, V., D. Lasry, Finite Element Simulation of Driver Folded Air Bag Deployment, SAE Paper No. 912904, 1991.
- [6] Lasry, D., R. Hoffmann, J. B. Protard, Numerical Simulation of Fully Folded Airbags and Their Interaction with Occupants with Pam-Safe, SAE Paper No. 910150, 1991.
- [7] Khalil, T. B., R. J. Wasko, J. O. Hallquist, D. W. Stillman, Development of a 3-Dimensional Finite Element Model of Air Bag Deployment and Interactions with an Occupant Using DYNA3D, SAE Paper No. 912906, 1991.

- [8] Yang, K. H., Y. Q. Li, Effects of the Airbag Folding Pattern in Out-of-Position Frontal Impact With an Airbag, AMD-Vol.169/BED-Vol. 25, Crashworthiness and Occupant Protection Systems, ASME 1993.
- [9] Materna, P., Advances in Analytical Modeling of Airbag Inflators, SAE Paper No. 920120, 1992.
- [10] Wang, J. T., Are Tank Pressure Curves Sufficient to Discriminate Airbag Inflators? SAE Paper No. 910808, 1991.
- [11] LS-DYNA3D (Non-linear Dynamic Analysis of Structures in 3 Dimensions) Theoretical Manual, Livermore Software Technology Corporation, 1994.
- [12] LS-DYNA3D (Non-linear Dynamic Analysis of Structures in 3 dimensions) User's Manual, Livermore Software Technology Corporation, 1995.
- [13] Wawa, J. C., S. J. Chandra, K. M. Verma, Implementation and Validation of a Finite Element Approach to Simulate Occupant Crashes with Airbags: Part I - Airbag Model, AMD-Vol. 169/BED-Vol. 25, Crashworthiness and Occupant Protection Systems, ASME 1993.
- [14] Wawa, J. C., S. J. Chandra, K. M. Verma, Implementation and Validation of a Finite Element Approach to Simulate Occupant Crashes with Airbags: Part II - Airbag Coupling with Crash Victim, AMD-Vol. 169/BED-Vol. 25, Crashworthiness and Occupant Protection Systems, ASME 1993.